

Analyzing the effects of *Drosophila* Zasp mutants in myofibril assembly.

José Luis Medina Quintana.

Department of Biology, McGill University, Montreal.

October 2024.

A thesis submitted to McGill University in partial fulfillment of the requirements of
the degree of Master of Science

©José Medina 2024

Content

Content	2
Table of Figures	4
Abbreviations / Terminology / Nomenclature	5
Abstract	7
Résumé	8
Acknowledgments	9
Contribution of Authors	10
Introduction	11
Literature review	15
Myofibril assembly: the role and function of the sarcomere, Z-discs, and Zasp protein family.	15
Evolutionary conservation of the sarcomere and the Zasp protein family in <i>Drosophila melanogaster</i> .	19
Zasp mutations in humans and their functional consequences.	23
The importance of <i>Drosophila</i> in myofibril assembly research: Insights from genetic studies.	28
Materials and methods.	32
Identification of human Zasp disease variants conserved on Zasp52.	32
Bioinformatic design for Zasp52-PR-607P>L.	36
Fly stocks and genetics.	38
Western analysis:	40
Determination of death stage.	40
PCR.	41
DNA extraction.	41
PCR primers.	41
PCR conditions:	44
Immunofluorescent staining and confocal microscopy.	45
Quantifications.	47
Electron microscopy	47
Yeast two-hybrid assay.	48
Plasmid construction.	48
Bacterial transformation, and mini-prep.	49
Yeast 2 Hybrid assay	49
Yeast mating	50
Results:	51
General aim 1: Design and analyze Zasp null mutants.	51

Design of Zasp52 null mutant: Flightless mutants and the absence of GFP and RFP preliminary confirms Zasp52 complete gene deletion.	51
Confirmation of Zasp52 null mutant: Western blot incubated with Zasp52 full-length antibody does not detect any isoforms in a Drosophila Zasp52 null mutant.	52
Confirmation of Zasp52 null mutant: Zasp52-designed primers amplify the Zasp52 gene in a wild-type sample, but no product is detected in the Zasp52 null mutant.	54
Confirmation of the Zasp52-Zasp67 double null mutant: Zasp67-designed primers amplify the Zasp67 gene in a wild-type sample, but no product is detected in the Zasp52-Zasp67 double null mutant.	57
Analysis of Zasp null mutants: Confocal microscopy of Zasp null mutants reveals severe IFM defects.	58
Quantifications of sarcomere length and sarcomere width reveal aberrant myofibril sizes in Zasp52 null mutants and Zasp52-67 double null mutants.	60
Transmitted electron microscopy confirms the aberrant phenotypes in Zasp52 null and Zasp52-67 double null mutant.	62
Zasp52-Zasp66 homozygous double null mutant and Zasp52-Zasp66-Zasp67 homozygous triple null mutant are lethal and die before third instar larvae.	64
General aim 2: Study the conservation of the Zasp function.	65
Anti-flag M2 antibody detected Flag fusion proteins in all the overexpression assays.	65
When Zasp52-PR is expressed by ACT88F-Gal4, the sarcomere presents overexpression defects, when the clinical variant “607P>L” is expressed, the phenotype worsens.	67
Quantifications of sarcomere length and sarcomere width on overexpression assays reveal statistically significant differences.	69
Confocal microscopy reveals that the rescue assays can partially rescue the 52 null mutants when Zasp52-PR and Zasp52-PR-607P>L are overexpressed.	70
Quantifications of sarcomere length and sarcomere width on rescue assays reveal myofibrils partially going back to wild-type sizes.	72
Yeast two-hybrid assays revealed an increase in binding affinity in Zasp52-PR-607P>L.	75
Discussion	77
Conclusion.	86
References.	87

Table of Figures

Figure 1	19
Figure 2	24
Figure 3	34
Figure 4	35
Figure 5	36
Figure 6	42
Figure 7	43
Figure 8	43
Figure 9	44
Figure 10	47
Figure 11	47
Figure 12	52
Figure 13	53
Figure 14	55
Figure 15	55
Figure 16	56
Figure 17	57
Figure 18	59
Figure 19	61
Figure 20	63
Figure 21	66
Figure 22	66
Figure 23	68

Figure 24	69
Figure 25	71
Figure 26	74
Figure 27	76
Figure 28	76

Abbreviations / Terminology / Nomenclature

aa: Aminoacids	A-band: Anisotropic band
ACM: Arrhythmogenic cardiomyopathy	Act88F : Actin 88F
ALP: Actinin-associated LIM protein	CRISPR: Clustered regularly interspaced short palindromic repeats
CTG: Curly, Green fluorescent protein	CyO: Curly, O
DM1: Myotonic Dystrophy 1	DTT: Dithiothreitol
DCM: Dilated cardiomyopathy	DLM: Dorsal longitudinal muscles
DMSO: Dimethylsulfoxide	DNA: Deoxyribonucleic acid
Dr: Drop	DVM: dorsoventral muscles
e.g: Example	EGTA: Ethylene glycol-bis(β -aminoethyl ether)-N,N,N',N'-tetraacetic acid
ENH: Actin-associated protein enigma homolog	FB-ID: FlyBase Identification number
FRT: short flippase recognition target	FWD: Forward
GFP: Green fluorescent protein	HCM: Hypertrophic cardiomyopathy
Hs-Flp: Heat shock flippase	HZaspI1: Human Zasp Isoform 1
HZaspI2: Human Zasp Isoform 2	I-band: isotropic band
IFM: Indirect flight muscles	kb: Kilobases

kDa: Kilo dalton	LDB3: LIM domain binding 3
LIM: LIN-11, Isl-1 and MEC-3	LVNC: left ventricular noncompaction
MFM: Myofibrillar myopathy	NCBI: National Center for Biotechnology Information
OR: Oregon Red (Wild type)	PAGE: Polyacrylamide Gel Electrophoresis
Pb: Pair bases	P-value: Probability value
PCR: Polymerase chain reaction	PDZ: Postsynaptic density protein, <i>Drosophila</i> discs large, and Zonula occludens-1 protein
PFA: Paraformaldehyde	RCM: restrictive cardiomyopathy
REV: Reverse	RFP: Red fluorescent protein
RNAi: Interference ribonucleic acid	SDS-PAGE: Sodium Dodecyl-Sulfate-Polyacrylamide Gel Electrophoresis
Sp: Sternopleural	T-test: Student's T-test
Ta: Annealing temperature	TEM: Transmitted electron microscopy
TFT: Tufted	TM: Melting temperature
TTG: Tm3, Green fluorescent protein	UAS: Upstream activating sequence
-WLHA:	- Tryptophan (W), Leucine (L), Histidine (H), Alanine (A). (Deficient media)
Y2H: Yeast two-hybrid assay	YMG: York Modified Glycerol
YPD: yeast extract peptone dextrose	Zasp: Z-disc Alternatively Spliced PDZ motif
Zasp FL: Zasp full-length antibody	ZM: Zasp motif

Abstract

The sarcomere is the basic contractile unit of muscle fibers bordered by Z-discs. In *Drosophila*, Z-disc structure and maintenance is mediated by actinin and the PDZ and LIM domain protein Zasp52, a structural component of Z-discs and a member of the Alp/Enigma protein family. Actinin is regarded as a central organizer of Z-discs because it cross-links actin filaments at the Z-disc; however, actinin null mutants do not completely disrupt the Z-disc structure in *Drosophila*. Previous reports have shown that Zasp52 can bind both actin and actinin, as well as itself, and Zasp52 may complement the function of actinin at the Z-disc. With this knowledge, the present works propose that the full scope of Zasp functions is likely hidden because of functional redundancy. To shed light on this, we have generated a CRISPR null mutant in Zasp52 for the first time, completely deleting the 50 kb genomic locus and presenting its phenotype in adult flies' indirect flight muscle. We also generated a double null mutant of Zasp52 and Zasp67, an Alp/Enigma family member exclusively expressed in indirect flight muscles. This work characterizes null mutants and shows how the Z-disc structure gets severely disrupted. Another reason the Zasp protein family has gained attention in the muscle field is its significance in muscle diseases when the protein members are mutated. We have studied and characterized the human disease variant "Zasp-608P>L" by expressing the exact ortholog of this disease variant "Zasp52-PR-607P>L" in the *Drosophila* indirect flight muscles. Our data suggest

molecular functions underlying human muscle disorders can be analyzed in *Drosophila*.

Résumé

Le sarcomère est l'unité contractile de base des fibres musculaires, délimitée par des disques Z. Chez la *drosophile*, la structure et le maintien des disques Z sont médiés par l'actinine et la protéine Zasp52, une composante structurelle des disques Z appartenant à la famille des protéines Alp/Enigma. L'actinine est considérée comme un organisateur central des disques Z car elle lie les filaments d'actine au niveau du disque Z ; cependant, les mutants dépourvus d'actinine ne perturbent pas complètement la structure du disque Z chez la *drosophile*. Des études antérieures ont montré que Zasp52 peut se lier à la fois à l'actine et à l'actinine, ainsi qu'à elle-même, et Zasp52 pourrait compléter la fonction de l'actinine au disque Z. Partant de cette idée, les travaux actuels ont émis l'hypothèse que l'ensemble des fonctions de Zasp nous est toujours inconnu, en raison de la redondance fonctionnelle. Pour clarifier cela, nous avons généré pour la première fois un mutant nul CRISPR de Zasp52, supprimant complètement le locus génomique de 50 kb et présentant son phénotype dans le muscle de vol indirect des mouches adultes. Nous avons également créé un double mutant nul de Zasp52 et Zasp67, un membre de la famille Alp/Enigma exclusivement exprimé dans les muscles de vol indirect. Ce travail caractérise les mutants nuls et montre comment la structure du disque Z est sévèrement perturbée. La famille de protéines Zasp a également attiré l'attention dans le domaine des maladies

musculaires lorsque les membres de la protéine sont mutés. Nous avons étudié et caractérisé la variante pathologique humaine « Zasp-608P>L » en exprimant l'orthologue exact de cette variante pathologique « Zasp52-PR-607P>L » dans les muscles de vol indirect de la *drosophile*. Nos données suggèrent que les fonctions moléculaires sous-jacentes aux troubles musculaires humains peuvent être analysées chez la *drosophile*.

Acknowledgments

I would like to acknowledge and thank those who made it possible for me to complete my Master's degree in biology at McGill, an accomplishment that a younger self would have thought was only a dream. First, my supervisor, Dr. Frieder Schöck, selected me into his lab and gave me the opportunity of my life. I thank him and the research associate, Dr. Anja Katzemich, for all the guidance, patience, understanding, and knowledge provided during the development of my research project; this experience has helped me immensely in my growth as a scientist. I want to thank my fellow Master's student Nikolai Ho, who collaborated with me repeatedly and shared experiences like attending the 2023 CanFly and 2024 European Muscle conferences. I thank my supervisory committee members, Dr. Nam-Sung Moon and Dr. David Dankort, who, through my committee meetings, provided a different viewpoint of my results and gave valuable insights. I want to acknowledge Marie-Pier Lalonde, who, during her undergraduate research project at Schöck's Lab, provided the first steps for the yeast-two-hybrid results contained in the present work. This research was possible thanks to the funding received

from various awards from McGill University and the CIHR and the generous stipend from my supervisor.

From a non-academic perspective, I dedicate this thesis to the memory of Heber Pérez Córdova, who, in a short time, became one of the most significant people in my life. His passing just as I began my Master's degree marked a profound loss. Before him, I had not known the depth of love I carried within me; after him, I found within myself an invincible resilience. He stood by me when I applied, celebrated with me when I received my acceptance letter and supported me through the delays and setbacks with my study permit. He watched me leave Mexico with joy, dreams, fears, and tears. Now, I hold onto dreams of someday sharing this accomplishment with him once more, somehow, somewhere. *"In the midst of winter, I found there was, within me, an invincible summer."* – Albert Camus *"The world is gone. I must carry you."* – Paul Celan.

Finally, but not less importantly, I want to thank my parents, Orlando Medina Guevara and Elizabeth Quintana Contreras, for always supporting and believing in my career; I know I would not be here without their faith in my career. To my friends who were supportive during my darkest times, when I thought I was not going to be able to make it, María Elena Carrillo Herrera and José Pablo Pérez Rascón.

Contribution of Authors

José Luis Medina Quintana entirely authored this thesis, with the help provided as outlined in the Acknowledgements section.

Introduction

Studying myofibril assembly is crucial for elucidating muscle development, maintenance of integrity, function, and the pathogenesis of muscle diseases. Of particular interest are sarcomeric proteins that when mutated cause muscle diseases, this is the case of the Zasp protein family. Zasp proteins play essential roles in Z-disc maintenance, but mutations in these proteins lead to cardiomyopathies and myofibrillar myopathies. Although the role of Zasp variants in disease is well-established, the underlying molecular mechanisms remain insufficiently understood. It has also been hypothesized that Zasp's roles in myofibril assembly may not yet be fully characterized.

The primary objectives of this study are to improve the understanding of the molecular mechanisms involved in myofibril assembly, with an emphasis on the Zasp protein family, and to provide insights into disease mechanisms.

The literature review in the next section shows the basis for this research project. It begins by outlining the key components of the research, including the structure of the sarcomere and its associated proteins, focusing on the Z-disc and the Zasp protein family, both of which are vital for myofibril assembly. The biological model organism *Drosophila melanogaster* is then introduced, highlighting the evolutionary conservation of sarcomeric structures and proteins compared to humans and the contributions of genetic studies in advancing muscle research. The review also addresses the current understanding of the *Drosophila* Zasp

family—Zasp52, Zasp66, and Zasp67—and their specific roles and mutant phenotypes, as well as known muscle diseases associated with mutations in the human Zasp gene. The essential role of *Drosophila* in providing insights into the Zasp protein family is emphasized. Unresolved questions, anticipated findings from this research, and potential therapeutic implications are also outlined.

The thesis is structured around two major aims: the design and analysis of *Drosophila* Zasp null mutants, and the investigation of the conservation of Zasp function. These aims are addressed in the research question: How do null mutations in the *Drosophila* Zasp family, along with the introduction of a human clinical variant in *Drosophila*, affect muscle development, function, and integrity, and to what extent do these findings demonstrate the conservation of molecular mechanisms between *Drosophila* and humans?

The first aim focuses on addressing the emerging roles of the Zasp protein family in muscle research. In humans, Zasp belongs to the ALP-Enigma family, which has seven members, while the *Drosophila* family comprises Zasp52, Zasp66, and Zasp67 (Fisher and Schöck., 2022). This work uses the term “Zasp protein family” to refer to both the human and *Drosophila* families. Due to the redundancy within these proteins, the full scope of the Zasp family’s functions may be obscured. In *Drosophila*, the three Zasp proteins bind key proteins such as actinin and actin, masking each other’s roles in mutant analysis (Liao *et al.*, 2016). The creation of Zasp-family null mutants could address these gaps in knowledge. However, the complex loci of these proteins have made it challenging to achieve this. This study focuses on the first-ever design and analysis of a Zasp52 null

mutant, the primary member of the *Drosophila* Zasp family. Characterizing this mutant, along with the Zasp52-Zasp67 double null mutant, establishes a foundation for future analyses of a complete Zasp null mutant, which could offer valuable insights into unresolved questions within the field of muscle biology. For instance, while actinin is considered a key Z-disc organizer, evidence suggests that an actinin null mutant does not fully disrupt myofibril assembly (Dubreuil and Wang., 2000; Fyrberg *et al.*, 1990). Also, Evidence on whether Zasp recruits actinin to the Z-disc is ambiguous (Katzemich *et al.*, 2013 versus Chechenova *et al.*, 2013). Depending on the phenotypes observed in the null mutants, it may be possible to argue that Zasp, rather than actinin, is the primary Z-disc organizer.

This first aim is divided into three sub-aims: 1a: Design and analysis of the Zasp52 null mutant. 1b: Design and analysis of the Zasp52-Zasp67 double null mutant. 1c: Determine the developmental stage at which lethality occurs in the Zasp52-Zasp66 double null mutant and the Zasp52-Zasp66-Zasp67 triple null mutant. Based on prior laboratory work, it is hypothesized that the Zasp52 null mutation will be viable but significantly impair *Drosophila*'s indirect flight muscles (IFMs). It is predicted that the Zasp52-Zasp67 double null mutant will exacerbate the phenotype more than the combined effects of the individual mutations while remaining viable. In contrast, the triple null mutant and the Zasp52-Zasp66 double null mutant are expected to be non-viable, requiring muscle analysis at embryonic stages. The Zasp52 null mutant and the Zasp52-Zasp67 double null mutant will be created via genetic crosses and analyzed through confocal and electron

microscopy, with sarcomere length and width measured to characterize the phenotype.

The second aim seeks to provide evidence of the high degree of conservation between the Zasp families of humans and *Drosophila*, aiming to establish a system for rapid investigation of muscle diseases involving clinical variants of the Zasp family. This work builds on prior research, where human Zasp isoform 1 was expressed in *Drosophila* indirect flight muscles, yielding an overexpression phenotype similar to that of the *Drosophila* Zasp52 isoform. This demonstrated a conserved mechanism of Z-disc and myofibril size control between humans and *Drosophila*. The next step is to test whether Zasp disease variants are similarly conserved. To date, nine amino acid point mutations in human ZASP have been unequivocally linked to cardiomyopathy and myopathy, as documented in the OMIM and MARRVEL databases (Sheikh *et al.*, 2007). Of these, four are either identical to or highly conserved in *Drosophila* Zasp52. This study begins by investigating one of these mutations, 608P>L, with plans to explore the remaining mutations in future research. Suppose this overexpression system proves effective in elucidating the molecular mechanisms underlying these Zasp point mutations. In that case, subsequent studies will extend the analysis to other members of the Zasp protein family, such as ALP and ENH. Following this, an extensive bioinformatic analysis will be performed to select allelic variants of human Zasp that are well-conserved in *Drosophila* Zasp52 to be evaluated. In ClinVar there are approximately 500 allelic variants of uncertain significance with the potential to be objects of study.

This second aim is divided into three sub-aims: 2a: Study Zasp52 transgenes carrying a mutation found in human patients (608P>L). 2b: Rescue the Zasp52 null mutant phenotype using Zasp transgenes. 2c: Investigate the potential molecular mechanism of the 608P>L mutation. This second general aim started with the alignment and sited modification of Zasp52 to carry the human 608P>L. On the *Drosophila* Zasp52, the conserved mutation is 607P>L, which we hypothesize will yield a distinct phenotype from the overexpression one obtained, reflecting disease conservation. This will be explored with the overexpression assays with Zasp52-PR and Zasp52-PR-607P>L by confocal microscopy and quantifications of sarcomere length and width. Rescue assays will attempt to recover the Zasp52 null mutant phenotype using Zasp52-PR, Zasp52-PR-607P>L, and a healthy human Zasp variant, with differences in rescue efficacy expected to provide further evidence of conservation. Finally, the Zasp-52-PR-607P>L mutation's effects on Zasp's binding affinity will be explored using Yeast Two-Hybrid assays.

Literature review

Myofibril assembly: the role and function of the sarcomere, Z-discs, and Zasp protein family.

Myofibril assembly is a complex and highly regulated process in which groups of proteins arranged in contractile units ensure the proper function of muscle fibers. Muscle fibers, or muscle cells, contain myofibrils, filamentous structures formed by

actin and myosin filaments. Each muscle fiber comprises hundreds of myofibrils arranged side by side in structures called sarcomeres. Sarcomeres, the basic contractile units of muscle, convert chemical energy into mechanical energy for muscle contraction. These myofibrils are defined by anisotropic (A-band) and isotropic (I-band) cross bands, giving muscle fibers their striated appearance (Franzini-Armstrong and Porter., 1963). These bands are defined regions characterized by the interaction of the filamentous proteins. The A-band contains myosin and actin filaments, while the I-band comprises the rest of the area where myosin is excluded. At the center of the I-band, actin filaments are anchored to the massive protein complex known as the Z-disc which borders the sarcomere. In the center of the sarcomere is the A-band where the actin filaments are excluded, and the myosin filaments are anchored to the M-line (H-zone) (Schöck and Gónzales-Morales., 2022). Proper assembly of myofibrils requires a complex system of protein interactions to arrange filaments into sarcomeric subunits, ensuring a consistent sarcomeric diameter essential for muscle assembly (Sanger *et al.*, 2005).

Despite the complexity of the myofibril assembly process, evidence suggests that studying this process can be simplified by focusing on the Z-discs and their associated proteins. Z-disc precursors (Z-bodies) are the first repetitive structures to appear in myotubes, and mutations in Z-disc-associated proteins result in the most severe myofibril assembly defects (Sparrow and Schöck., 2009). Research on Z-discs, described as "one of the most complex macromolecular structures in biology" (Knöll *et al.*, 2011), has advanced significantly in the past two

decades. Once considered important solely for mechanical stability, Z-discs are now recognized as key to understanding myofibril assembly (Knöll *et al.*, 2011; Schöck and Gónzales-Morales., 2022; Pyle and Solaro., 2004; Luther., 2009; Frank *et al.*, 2006). Schöck and Gónzales-Morales (2022) provide a detailed analysis of the additional roles of Z-discs, which include coordinating sarcomere maintenance, serving as an enzymatic hub, and organizing actin filaments. The growing recognition of the Z-disc's importance in muscle research has extended to its role in disease, particularly with the discovery of disease variants of major Z-disc proteins that cause various muscular dystrophies, collectively termed "Z-discopathies" (Frank *et al.*, 2006; Knöll *et al.*, 2011; Wadmore *et al.*, 2021). This underscores the significance of Z-discs and their associated proteins in muscle research. One such protein, the Zasp family, will be the main focus of this study.

The ALP/Enigma proteins are strongly associated with animal muscles and movement. These proteins bind to cytoskeletal proteins, facilitating the rearrangement and reorganization of the cytoskeleton required for muscular contraction (Krcmery *et al.*, 2013). Characterized by the presence of a PDZ domain, LIM domains, a ZM (Zasp motif) domain, and an AM (ALP motif) domain, this protein family includes seven members in vertebrates (ZASP, ALP, Enigma, CLP-36, Mystique, RIL, ENH) and three in *Drosophila* (Zasp52, Zasp66, and Zasp67). Probably, the best-documented member in vertebrates is Zasp (Z-disc associated alternatively spliced protein – LDB3 gene), a core protein of the Z-disc. Zasp in vertebrates contains a PDZ domain at its N-terminus, three LIM domains at its C-terminus, and a ZM, (Fisher and Schöck., 2022). Human Zasp contains 16

exons, giving rise to six reported isoforms highly expressed in striated muscle. These isoforms are alternatively spliced as those that possess exon 4 are expressed in cardiac tissue, while those having exon 6 are more highly expressed in skeletal muscle (Waldmore *et al.*, 2021). Zasp, in both biological systems, is known to be a sarcomeric protein that interacts with Z-disc-associated proteins, including α -actinin, which is considered the main Z-disc organizer in current muscle research (Fratev *et al.*, 2014; Dubreuil and Wang., 2000). This interaction is crucial for maintaining the structural integrity and function of the sarcomere, highlighting the significance of Zasp proteins in muscle biology and research.

The Zasp protein family has more functions than previously appreciated in muscle research, and the full scope of their roles in myofibril assembly is likely underexplored. In mammals, Zasp is essential for Z-disc maintenance, organizing actin stress fibers, and providing actin anchorage (Miyazaki *et al.*, 2012; Pashmforoush *et al.*, 2001; Zheng *et al.*, 2010). Recent data suggest even broader roles, including regulating Z-disc growth and the initial steps of Z-body assembly (González-Morales *et al.*, 2019b, Katzemich *et al.*, 2011, Nikonova *et al.*, 2020). Additionally, like the Z-disc, Zasp is undergoing a reevaluation concerning its role in muscle diseases, with disease-associated Zasp variants linked to various myopathies such as dilated cardiomyopathy (DCM), left ventricular noncompaction cardiomyopathy (LVNC), hypertrophic cardiomyopathy (HCM), and myofibrillar myopathy (MFM) (Fratev *et al.*, 2014). Understanding the Zasp group of proteins is crucial, as unraveling the molecular mechanisms of Zasp will enhance the understanding of myofibril assembly dynamics and provide insights into muscle

disease mechanisms. This research aims to contribute to this understanding, highlighting the importance of Zasp in muscle biology and pathology.

Evolutionary conservation of the sarcomere and the Zasp protein family in *Drosophila melanogaster*.

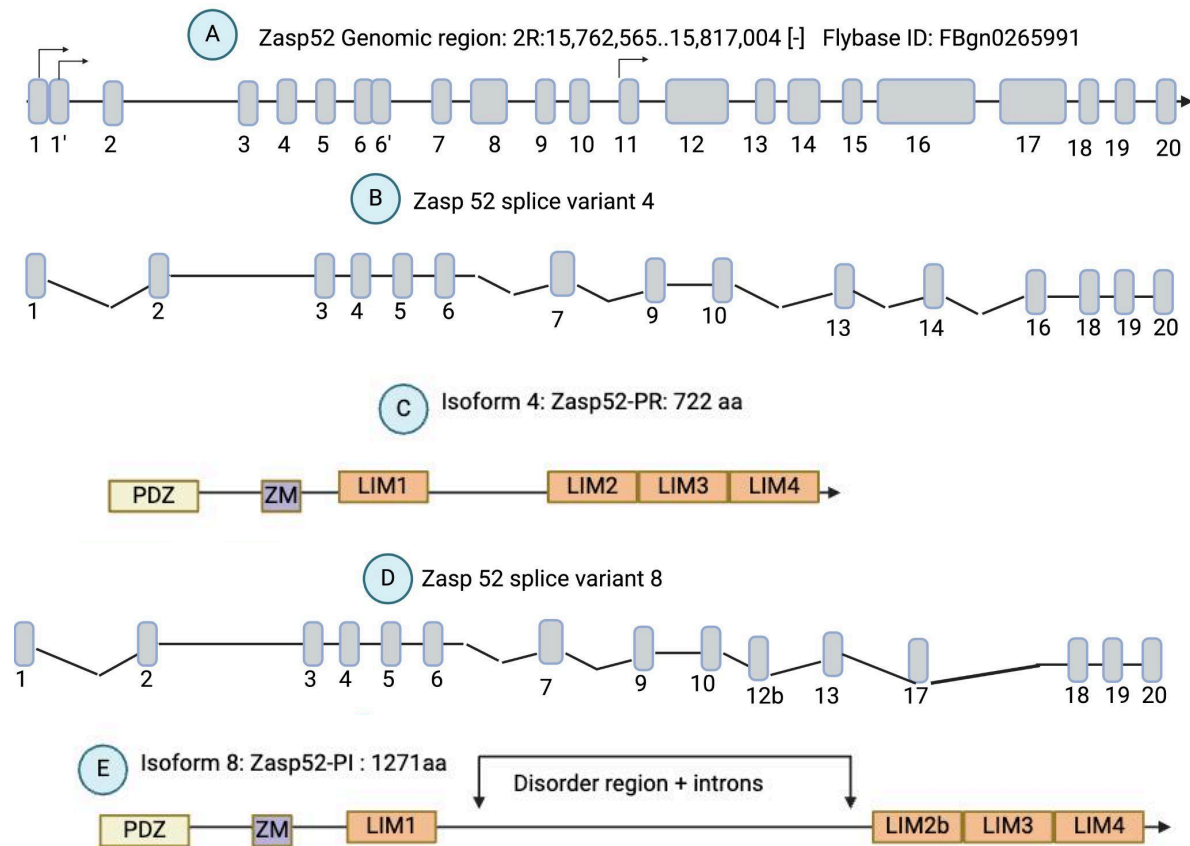


Figure 1: Zasp52 gene model. Arrows indicate alternative start sites. A) Full genomic region with its 22 annotated transcripts. B) The most common isoform encoded by splice variant four, which will be used in the present work. C) Functional domains and length encoded by the most common isoform,

“Zasp52-PR”. D) Isoform exemplifying alternative splicing of LIM domains, encoded by splice variant 8. E) Functional domains, additional disorder regions, and Zasp52-RI length encoded by splice variant 8. The figure was made by the author in Biorender, based on Flybase: FBgn0265991, and Katzemich *et al.* (2011).

Due to the high degree of conservation in muscles, *Drosophila melanogaster* serves as an ideal biological model for myofibril assembly research. Muscles can be traced back to the emergence of eumetazoans, which include bilateral animals and cnidarians (Burton, 2008; Seipel and Schmid, 2005). The sarcomere exemplifies nature's reuse and repurposing of biological structures throughout evolution, as sarcomeres are highly conserved in all bilaterian animals (Steinmetz *et al.*, 2012; Poovathumkadavil and Jagla, 2020). This conservation is evident in higher insects like *Drosophila*, which owes its extraordinary flight capabilities to indirect flight muscles (IFMs) attached to the thorax. IFMs consist of two muscle groups: the dorsoventral muscles (DVMs) and the dorsal longitudinal muscles (DLMs), which provide the necessary power for contraction to indirectly move the *Drosophila* wings (Gunage *et al.*, 2017). Several studies highlight that similarities begin with the formation of skeletal muscle tissue during embryonic development, known as myogenesis (Maqbool and Jagla., 2007; Poovathumkadavil and Jagla., 2020; Bate., 1990; Abmayr *et al.*, 1995; Ciglar and Furlong., 2009). *Drosophila* myogenesis leads to the formation of vertebrate-like multi-fiber muscle, exhibiting a fibrillar organization and resulting in the characteristic voluntary, syncytial, and striated skeletal muscles that closely resemble those of vertebrates (Poovathumkadavil and Jagla., 2020). Thus,

Drosophila IFMs are well-researched striated muscles with a highly regular sarcomere structure, which will be a primary focus of the present research.

Despite notable structural differences in muscles between *Drosophila* and vertebrates, both share similar locomotory behaviors due to conserved sarcomere structures, associated genes, pathways, and processes (Poovathumkadavil and Jagla., 2020). Approximately 60% of *Drosophila* genes have human orthologs (Rubin., 2001), and about 75% of the genes responsible for human diseases have homologs in flies (Ugur *et al.*, 2016). This conservation is evident in the Alp/Enigma family, where functional domains are preserved across species. The simpler genetic structure in *Drosophila*, with only three Alp/Enigma family members (Zasp52, Zasp66, and Zasp67), simplifies genetic modifications and interpretations making it an effective model for muscle research.

Zasp52, a major *Drosophila* Zasp PDZ domain protein, colocalizes with α -actinin at the Z-discs and encodes at least 22 isoforms and 61 proteins, with some expressed exclusively in the IFMs (Katzemich *et al.*, 2011; Nikonova *et al.*, 2020; González-Morales *et al.*, 2019a). Zasp66 and Zasp67, arising from duplications in early and higher insects respectively, cooperate with Zasp52 in myofibril assembly, playing redundant roles at the Z-disc (Katzemich *et al.*, 2013; González-Morales *et al.*, 2019b). Zasp52 contains an N-terminal PDZ domain, a weakly conserved ZM domain, and four LIM domains, unlike its human ortholog, which has three. Zasp66 and Zasp67 retain PDZ and ZM domains but lack LIM domains. The PDZ domain, a prevalent interaction module, is crucial for myofibril assembly, interacting with α -actinin, while the LIM and ZM domains mediate

self-interaction for Z-disc growth (Liao *et al.*, 2020). Recent studies suggest that Alp-Enigma shorter isoforms (one or no LIM domains) limit Z-disc growth. In contrast, longer isoforms (three or four LIM domains) promote it, both in mammals and *Drosophila*. González-Morales *et al.*, (2019b) identified some Zasp52 isoforms as "growing" and Zasp66 and Zasp67 as "blocking" isoforms. The balance between these isoforms maintains the consistent diameter of *Drosophila* Z-discs, with imbalances leading to pathological aggregate formation, a hallmark of myopathies.

Parallel patterns are evident in humans, where Zasp isoforms without LIM domains may act as blocking isoforms (Fisher and Schöck., 2022). In mice, knockout of larger Zasp isoforms leads to Z-disc perturbations and lethality, while knockout of shorter isoforms yields no phenotype (Cheng *et al.*, 2011). Katzemich *et al.*, (2011) identified 13 Zasp52 splice variants, among which Zasp52-PR is particularly interesting in this study (See Figure 1B-C). As the most common isoform, encoded by splice variant 4 (FB-ID: FBpp0302946), Zasp52-PR is a long/growing isoform of 722 amino acids, containing all functional domains but lacking disordered regions; it is also the direct ortholog of Human-Zasp-Isoform1. Another critical feature of Zasp52 is the splicing pattern of LIM domains. Zasp52 exons encoding domains can be alternatively spliced to give rise to six different LIM domains (Katzemich *et al.*, 2011). As shown in Figure 1D-E) the LIM2 domain can be encoded either by exon 16 (LIM2) or exon 17 (LIM2b); this difference has an impact later in this work in the Yeast two-hybrid assay. Investigating the

Drosophila Zasp family thus offers valuable insights into both normal and abnormal muscle development, with potential implications for human muscle research.

Zasp mutations in humans and their functional consequences.

Mutations in Zasp are becoming a critical aspect of muscle research due to their strong association with muscle disease. MFMs are skeletal muscle diseases characterized by diverse clinical features but a similar morphological phenotype. At the molecular level, this phenotype is associated with the disintegration of myofibrils, Z-disc dissolution, accumulation of degradation products, and expression of ectopic proteins (Selcen and Engel., 2011). Clinically, patients experience chronic muscle degeneration, leading to muscle weakness, joint contractures, partial or total loss of movement, and muscle atrophy, among other common symptoms (Wadmore *et al.*, 2021). The significance of Zasp in MFM is underscored by the recent change of name in this subtype of disease as “Zaspopathies”, referring to any autosomal dominant form of skeletal muscle dystrophy genetically marked by a Zasp single aminoacidic substitution (Sheikh *et al.*, 2007; Griggs *et al.*, 2007; Selcen and Engel., 2005). As mentioned, Zasp follows an alternative splicing pattern that generates different isoforms with tissue-specific expression patterns, which is relevant to the role of Zasp in disease. For instance, Zaspopathies are predominant when the skeletal-specific exon 6 is the mutated locus (Wadmore *et al.*, 2021). Furthermore, Zasp mutations have been linked to various cardiomyopathies, a heterogeneous group of diseases affecting the heart muscle's structure and function (Bang *et al.*, 2022). Cardiomyopathies

impair the heart's ability to pump blood effectively and are classified as hypertrophic cardiomyopathy (HCM), dilated cardiomyopathy (DCM), restrictive cardiomyopathy (RCM), arrhythmogenic cardiomyopathy (ACM), and left ventricular noncompaction (LVNC) (Bang *et al.*, 2022). The mutated loci of Zasp influence the disease variant in cardiomyopathies, particularly the cardiac-specific exon 4, though exon 6-point mutations can also cause cardiomyopathy forms. In summary, the recent trend of recognizing additional functions of Zasp has significantly impacted muscle research and helped define a new group of diseases.

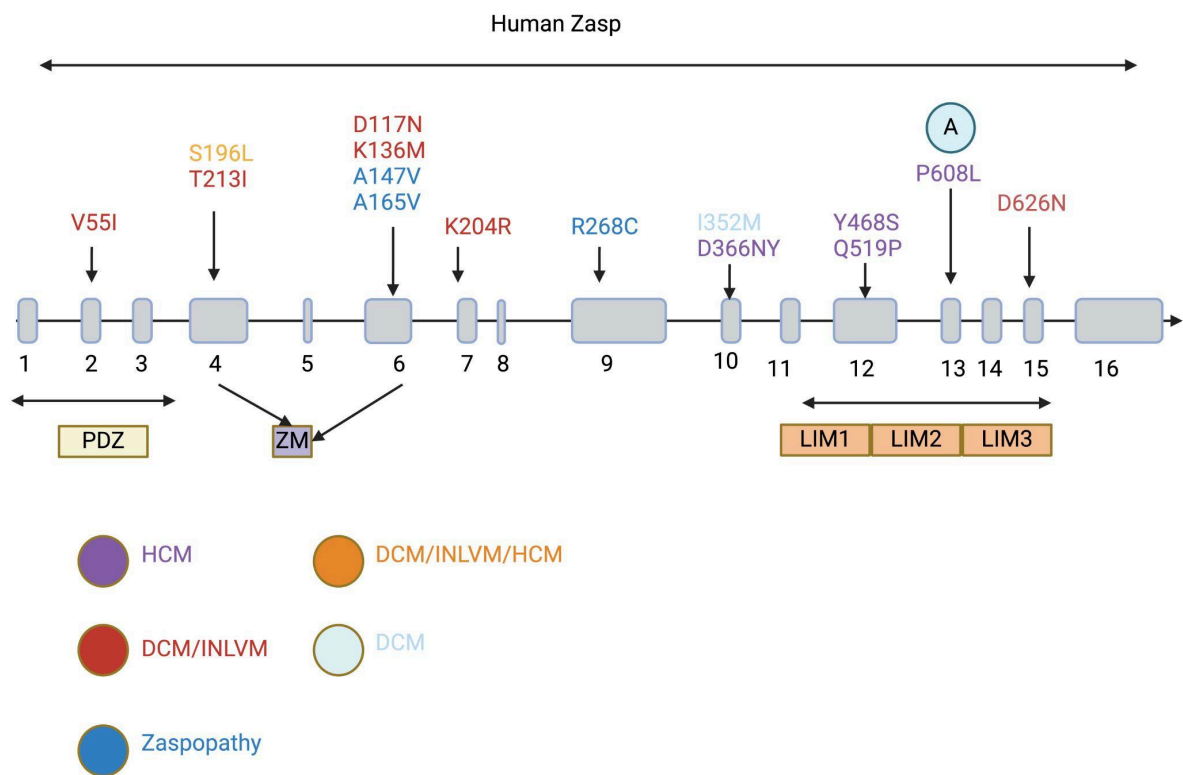


Figure 2: Human Zasp gene model. Genetic organization with identified mutations in different colors depending on the associated diseases. HCM: Hypertrophic cardiomyopathy DCM: Dilated cardiomyopathy INLVM: Isolated

noncompaction of the left ventricular myocardium. Functional domains affected are also shown. The last exon of the short human Zasp isoform; Exon 16: The last exon of the long human Zasp isoform. A) Human Zasp-608P>L showed. This figure was done using Biorender, adapted from Sheik. *et al.*, 2007.

The first findings about Zasp mutants have helped to link disease variants with poorly understood myopathies. Pinpointing the exact starting point of this trend is challenging, however, one of the first and most influential studies was published by Zhou *et al* in 2001. The authors designed a Zasp-knock-out mutant mouse, ablated at least Zasp1 and Zasp2, resulting in perinatal lethality, with survivors dying within the first five days. This lethality was linked to functional failure in multiple striated muscle types, exhibiting symptoms of congenital myopathies such as cyanosis, gasping respiratory patterns, limb weakness, and defective locomotory behavior. Electron microscopy of these mice revealed severely disrupted cardiac muscle and disorganized Z-discs. Zhou *et al.*'s work led to the subsequent discovery of Zasp mutations in human patients, with the first disease variants identified in familial and sporadic dilated cardiomyopathy (Arimura *et al.*, 2004; Vatta *et al.*, 2003). In their review, Sheikh *et al.* (2007) discussed the first clinically significant point mutations in human Zasp. Figure 2 represents 15-point mutations addressed by the authors, classified by disease type (cardiomyopathy: DCM, HCM, INLVM) or Zaspopathy, and the mutated functional domain. One of these mutations, "P>L608" (Figure 2-A) was chosen for this research, affecting the LIM3 domain and causing HCM. Mutations in the LIM domains are particularly interesting due to their implications in pathological processes. These first research

works lay out the interest in identifying Zasp disease variants, linked with specific phenotypes.

Following the identification of disease-causing human Zasp mutations, recent studies have concentrated on exploring the underlying molecular mechanisms. For example, Lin *et al.* (2014) investigated the 165A>V and 147A>T mutations in Zasp, located in the exon-6 encoded ZM domain in all human isoforms. Their research validated the crucial role of Zasp isoforms in skeletal muscles, finding that only the “ZASP-Lex10” isoform, which lacks exon 10, exhibited disrupted effects of the 165A>V and 147A>T Zasp mutants in cultured mouse cells. After testing various alternatively spliced isoforms, the authors concluded that the actin-binding region of ZASP-Lex10 (with exon 10 deleted) is essential for the aberrant actin phenotype of both mutants. Similarly, Selcen and Engel., (2005) studied the 165A>V mutation using knock-in mice to investigate the disease mechanism. The human Zasp point mutation was introduced in the mouse Zasp isoform (CIPHER) with over 92% amino acid homology. Immunostaining of serial muscle sections in these mice revealed that the point mutation induced protein aggregates of filamin C and its chaperones by disrupting signaling pathways responsible for the disposal of damaged cytoskeletal components. This study highlighted additional roles of Zasp, demonstrating that Zasp acts as a major mechanosensory hub in the Z-disc of skeletal muscle. In another study, the third LIM domain human Zasp point mutation 626-D>N was examined after being detected in a familial case of dilated cardiomyopathy (DCM) (Arimura *et al.*, 2004). Using a yeast two-hybrid assay (Y2H), the authors proposed that the mutation

increases the binding affinity with protein kinase C (PKC). Fratev *et al.*, (2014) suggested a similar disease mechanism in their research on the G54S point mutation, a variant classified as having unknown significance. This mutation, the first PDZ domain mutation potentially linked to HCM, was studied using bioinformatics, molecular dynamics, and free energy calculations to assess its structural impact. The *in silico* structural results indicated a reduction in binding affinity between the Zasp disease variant and target proteins such as α -actinin2 and the LTCC. As shown, the more research conducted on Zasp mutants in the muscle field, the more roles of Zasp and associated disease mechanisms are discovered.

Over the last two decades, significant advances have been made in Zasp research; however, there remains a considerable journey towards properly diagnosing and treating Zasp-related myopathies. Knoll's (2011) review highlights that, in vertebrates, studies have investigated the knockout of most Alp-Enigma family proteins individually, resulting in different phenotypes. For example, Zasp null mice, discussed in this literature review (Zhou *et al.*, 2001), led to the conclusion that Zasp is not required for myofibrillogenesis or Z-disc maturation, a point also noted by various authors (Knoll *et al.*, 2011; Frank *et al.*, 2006; Sheik *et al.*, 2007). Nevertheless, the Alp-Enigma family consists of seven different members with multiple spliced variants, suggesting a high potential for functional redundancy. Knoll's (2011) review also emphasizes that there is no defined disease-causing molecular mechanism for most observed knockout animals or patients with Alp-Enigma disease variants. A common theme among the works

mentioned in this section is the obscure disease mechanisms underlying most Zasp-related myopathies. A true Alp-Enigma null mutant could address these unanswered questions, but it has not yet been possible to knock down all family members in mammals. The present work provides fundamental steps toward analyzing a complete Alp-Enigma null mutant for the first time, which could lead to a deeper understanding and better treatment of Zasp-related myopathies.

The importance of *Drosophila* in myofibril assembly research: Insights from genetic studies.

The expanded role of Zasp52 in *Drosophila* has provided significant insights into muscle research. The Schöck Lab discovered Zasp52 while investigating novel genes required to maintain and develop functional integrin adhesion sites (Jani and Schöck., 2007; Rohn *et al.*, 2011). These studies extended Zasp's function beyond Z-disc maintenance. In their article review, Fisher and Schöck (2022) highlighted additional roles, such as being a core regulator of Z-disc, integrin activation, and cell signaling regulation during contraction. Katzemich *et al.*, (2013) demonstrated that Zasp52 is one of the first Z-disc markers in IFM development, revealing an indispensable role already in Pupal Myofibril Development. Liao *et al.*, (2016) characterized the binding relationship between Zasp and α -actinin, identifying the PDZ domain plus a 35 amino acid C-terminal extension as crucial for this interaction. This result from the authors is consistent with vertebrates, and they proposed to coin the term “Zasp PDZ domain proteins” for all proteins containing the conserved PWFFRL in the N-terminal half of PDZ, to improve the classification

of the Zasp protein family and add new members with very similar domain structure. Finally, Liao *et al.*, (2020) showed that Zasp52 also directly binds actin filaments. These findings illustrate the broader functional significance of Zasp52 in muscle development and maintenance in *Drosophila*. Similar to the human Zasp ortholog, muscle research advances have consistently translated into more Zasp52 functions.

The discovery and characterization of Zasp52 in *Drosophila* led to the identification of other family members, Zasp66 and Zasp67, improving the understanding of the Zasp protein family. Katzemich *et al.* (2013) identified Zasp66 and Zasp67 through a detailed database search for Zasp PDZ domain proteins in *Drosophila* and humans. They found that Zasp52 and Zasp66 act together in the assembly stages by binding to α -actinin, a finding consistent with the expression pattern characterized by González-Morales *et al* (2019a). Zasp66 co-localizes with Zasp52 during embryonic and pupal myofibril assembly, while Zasp67 is exclusively expressed during the pupal stages (FlyBase). The characterization of Zasp66 and Zasp67, including the creation of null mutants through CRISPR-mediated homology-directed repair, provided significant insights. González-Morales *et al.* (2019a) designed null mutants by the insertion of genetic cassettes that replaced exons 2,3, and 4; then the authors confirmed the nulls by PCR amplification of the cassettes and, at the same time lack of amplification when targeting the deleted exons. The CRISPR Zasp67 homozygous null mutant is completely flightless, while the Zasp66 homozygous null mutant shows high pupal lethality but does not affect flying. Double mutants analyzed by Katzemich *et al.*

(2013) and González-Morales *et al.* (2019b) demonstrated more severe phenotypes, indicating the combined effects of mutating two Zasp proteins are more severe than the additive defects of single mutants. These findings highlight the functional redundancy and interdependent roles of Alp/Enigma family members in *Drosophila*, emphasizing the complexity of Z-disc and myofibril assembly.

Creating an Alp-Enigma null mutant is essential to resolve critical debates in muscle research. The role of α -actinin as a central organizer of Z-discs is debated. While Z-disc formation fails without the α -actinin binding domain in IFMs (Sparrow *et al.*, 1991), α -actinin null mutants exhibit muscle function and integrity before dying (Dubreuil and Wang, 2000; Fyrberg *et al.*, 1990). This suggests α -actinin's importance in sarcomere maintenance over initial assembly. The Schöck Lab proposes that the Zasp protein family could be the potential central organizers of Z-discs. Creating a null mutant is expected to completely abolish Z-disc formation and myofibril assembly. Additionally, there is debate over whether Zasp recruits α -actinin to the Z-disc. Hypomorphic mutants studied using RNAi have yielded conflicting results, with Chechenova *et al.* (2013) showing loss of α -actinin localization and Katzemich *et al.* (2013) showing normal localization. These conflicting results highlight the need for a complete Zasp null mutant to fully understand the protein family's functions and address redundancy issues. In vertebrates, only double null mutants have been analyzed (Mu *et al.*, 2015), while *Drosophila*, with only three family members, offers a more simple genomic interpretation. The Schöck Lab has already analyzed complete null mutants for Zasp66 and Zasp67 (González-Morales *et al.*, 2019b), in addition to Zasp52 alleles

which separately affect the protein domains and truncate several Zasp52 isoforms (Katzemich *et al.*, 2013, Liao *et al.*, 2016).

Nevertheless, the large and complex locus of Zasp52 has prevented the creation of a complete Zasp null mutant in *Drosophila*. This work will focus on continuing these efforts to achieve a complete triple null mutant in *Drosophila*. Addressing these debates by creating a complete Zasp null mutant will clarify the roles of these proteins in muscle biology, providing insights that are critical for understanding muscle development and maintenance.

Drosophila is a biological model that has successfully recapitulated key hallmarks of typical human muscle diseases characterized disease mechanisms, and even provided potential therapy venues. One notable example is the modeling of Myotonic Dystrophy 1 (DM1), where a *Drosophila* model mimicked the hypercontraction phenotype of myotonia patients caused by a CTG abnormal repeat expansion, contributing to the characterization of the disease (Picchio, *et al.*, 2013). In another DM1 study, García-Lopez *et al.*, (2011) identified 15 genetic modifiers of CUG-induced toxicity, improving disease phenotypes and pointing to potential therapy venues. Similarly, research on Z-disc diseases like Zaspopathies and cardiomyopathies has used *Drosophila* to reveal conserved disease mechanisms. For instance, the study of the *Drosophila* co-chaperone Starvin (Stv) and its human ortholog BAG-3 (mutated BAG-3-209P>L causes childhood myopathy) demonstrated Z-disc disruption and muscle weakness in both species, linking the condition to chaperone-assisted selective autophagy (CASA) impairment (Arndt *et al.*, 2010). *Drosophila* has also been used to model

cardiomyopathies, successfully replicating structural and functional defects observed in human conditions like increased chamber size and reduced systolic dysfunctions (Zhao *et al.*, 2023). This is of critical importance as the point mutation that will be studied here (608P>L) is known to cause familial hypertrophic cardiomyopathy. These models have established genetic causality for dilated cardiomyopathy (Luso *et al.*, 2018), a rare form of severe infantile cardiomyopathy (Migunova *et al.*, 2021), and hypertrophic cardiomyopathy of infantile-onset (Manivannan *et al.*, 2020), highlighting the significance of *Drosophila* in muscle disease research. This work aims to characterize a Zasp clinical variant using a transgene overexpression assay, potentially providing a system to evaluate the function of clinical variants and identify disease-causing mutations.

Materials and methods.

Identification of human Zasp disease variants conserved on Zasp52.

Figure 2 illustrates the 15 pathogenic point mutations identified in the human Zasp protein. To determine which mutations aligned with this study, I performed a sequence alignment of human Zasp and *Drosophila* Zasp52 proteins using BlastP in NCBI.

Human Zasp aminoacid sequence (Uniprot: O75112):

MSYSVTLTGPGPWGFRLQGGKDFNMPLTISRITPGSKAAQSQLSQGDLVVAIDGV
NTDTMTHLEAQNKIKSASYNLSLTLQKSKRPIPISTTAPPVQTPLPVIPHQKDPALD

TNGSLVAPSPSPEARASPGTPGTPELRPTFSPAFSRPSAFSSSLAEASDPGPPRAS
LRAKTSPEGARDLLGPKALPGSSQPRQYNNPIGLYSAETLREMAQMYQMSLRGK
ASGVGLPGGSLPIKDLAVDSASPVYQAVIKSQNKPEDEADEWARRSSNLQSRSF
RILAQMTGTEFMQDPDEEALRRSSTPIEHAPVCTSQATTPLLPAQAQPPAAASPSA
ASPPLATAAAHTAIASASTTAPASSPADSPRPQASSYSPAQAASSAPATHTSYSEGP
AAPAPKPRVTTASIRPSVYQVPASTYSPSPGANYSPTPYTPSPAPAYTPSPAPA
YTPSPVPTYTPSPAPAYTPSPAPNYPAPSVAYSGGPAEPASRPPWVTDDSFQK
FAPGKSTTSISKQTLPRGGPAYTPAGPQVPPLARGTVQRAERFPASSRTPLCGHC
NNVIRGPFLVAMGRSWHPPEEFTCAYCKTSLADVCFVEEQNNVYCERCYEQFFAP
LCAKCN TKIMGEVMHALRQTWHTTCFVCAACKKPF GNSLFH MEDGE PYCEKDYI
NLFSTKCHGCDPVEAGDKFIEALGHTWHDTCFICAVCHVNLEGQPFYSKKDRPL
CKKHAHTINL

Zasp52-PR aminoacid sequence (Flybase: FBgn0265991)

MAQPQLLQIK LSRFDAQPWG FRLQGGTDFA QPLLQKVNA GSLSEQAGLQ
PGDAVVKINDVDVFNLRHKD AQDIVVRSGN NFVITVQRGG STWRPHVTPT
GNVPQPNSPY LQTVTKTSLAHKQQDSQHIG CGYNNAARPF SNGGDGGVKS
IVNKQYNTPV GIYSDESIAE TLSAQAEVLGGVLGVNFKK NEKEYQGDRS
EVLKFLREEE TGQSTPAFGN SHYEHDAQQ LQQPQQQYNQHQQHYHQQQQ
QQQSSTTRHV SAPVNSPKPP STGGLPTGQN ICTECERLIT GV FVRIKDN
LHVECFKCAT CGTSLKNQGY YNFNNKLYCD IHAKQAANN PPTGTEGYVP
VPIKPNTKLSASTISSALNS HGYGGHSGY SNGNSTPAPA PVNQGYARPF
GAAAPKSPVS YPPQQQQQSPRPAPGGQNPY ATLPRSNVGQ QGRNVRYQQQ
QQQQQQYNNQ QKQQYRNSYP MGSNYSTPSQSPYITSNTNN YSSNSYNNN
NYSNYNNNNV YRGAGGKSAG AFGATSAPKR GRGILNKAAGPGVRIPLCNS
CNVQIRGPFI TALGRIWCPD HFICVNGNCR RPLQDIGFVE EKGDLYCEYC
FEKYLAPTCS KCAGKIKGDC LNAIGKHFHP ECFTCGQCGK IFGNRPFFLE
DGNAYCEADWNELFTTKCFA CGFPVEAGDR WVEALNHNYH SQCFNCTFCK
QNLEGQSFYN KGGRPFCNHR

The BlastP analysis identified regions of amino acid sequence conservation between human Zasp and *Drosophila* Zasp52. As shown in Figure 3, proline 608 exhibits a perfect match between the two sequences. This residue, located within the conserved LIM domain, was selected as the primary focus for further study due to its functional relevance and pathogenic association. In addition to the P>L608 mutation, three other point mutations from Figure 2—V55I, A147V, and T213I—are also highly conserved between the two systems. These mutations are highlighted in Figure 4.

Sequence ID: **Query_2018885** Length: **728** Number of Matches: **5**

Range 1: 534 to 727 [Graphics](#) [Next Match](#) [Previous Match](#)

Score	Expect	Method	Identities	Positives	Gaps
223 bits(567)	6e-67	Compositional matrix adjust.	96/196(49%)	124/196(63%)	4/196(2%)
Query 538	PPLARGTVQRAERFPASSRTPLCGH	CNNVIRGPFLVAMGRSWHP	EEFTC--AYCKTSLAD	595	
Sbjct 534	P KRGRGILNKAA--GPGVRI	R PLC CN IRGPF+ A+GR W P+ F C C+ L D	591		
Query 596	VCFVEEQNNVYCERCYEQFFAPLCAK	CNTKIMGEVMHALRQTWH	TCFVCAACKKPF	GNS 655	
Sbjct 592	IGFVEEKGDLYCEYCFEKLAPTCSK	CAGKIKGDCLNAIGKHFH	PECFTCGQCGKIF	GNR 651	
Query 656	L FHMEDGEPEYCEKDYINLFSTK	CHGCDPVEAGDKFIEALGHTW	HDTCFICAVCHVN	LEG 715	
Sbjct 652	PFFLEDGNAYCEADWNELFTTKC	FACGFPVEAGDRWVEALNHN	YHSQCFNCTFCKQ	NLEG 711	
Query 716	QPFYSKKDRPLCKKHA	731			
Sbjct 712	QSFYNKGGRPFCKNHA	727			

Figure 3:Results of the alignment between human Zasp (query) and *Drosophila* Zasp52 (subject) using NCBI BlastP. The alignment identified five conserved regions; this figure highlights one such region (amino acids 534–727). The purple arrow marks the conserved residue P608, which is present in both systems.

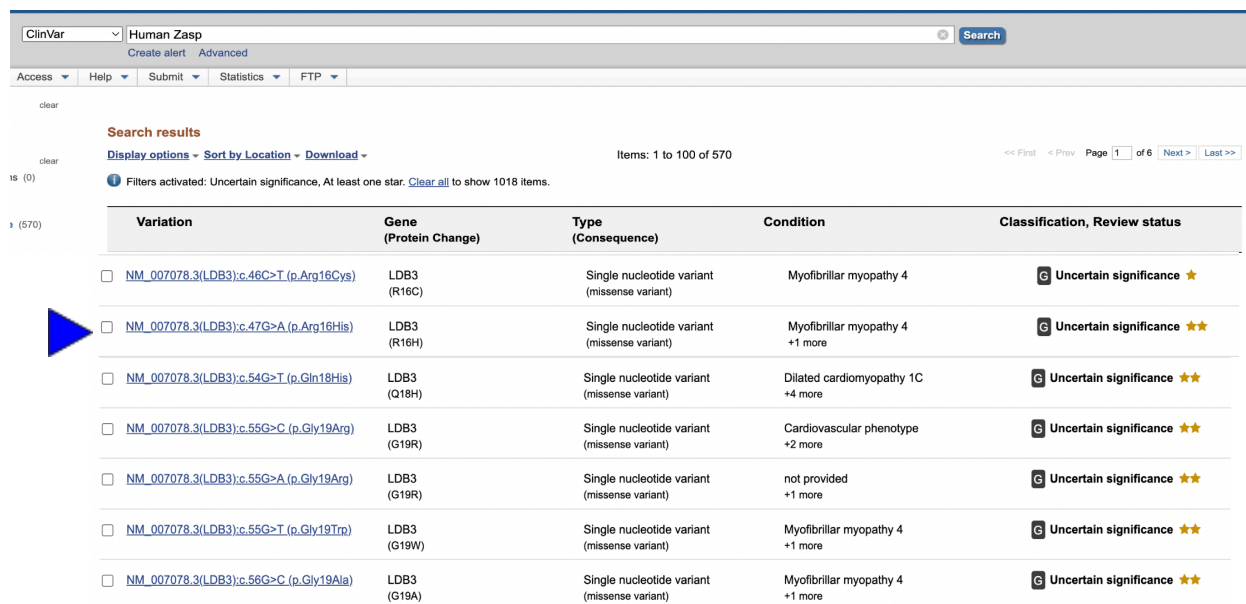
Range 2: 18 to 188 [Graphics](#) [▼ Next Match](#) [▲ Previous Match](#) [▲ First Match](#)

Score	Expect	Method	Identities	Positives	Gaps
73.2 bits(178)	2e-1	Compositional matrix adjust.	58/216(27%)	93/216(43%)	45/216(20%)
Query 12	PWGFR	LQGGKDFNMPLTISRITPGSKAAQSQLSQGDLVVAIDGVNTDTMTHTLEAQNKIKS	71		
Sbjct 18	PWGFR	LQGG DF PL + ++ GS + Q+ L GD VV I+ V+ + H +AQ+ +	77		
Query 72	ASYNLS	LTQKSKRPIPISTTAPPVQTPLPVIPHQKDPALDTNGSLVAPSPSPPEARASPG	131		
Sbjct 78	SGNNF	VITVQRG-----GSTWRPHVTPGTGNVPQPNSPYLQT---VTKTSLAHKQQDS--	126		
Query 132	TPGTPE	LRPTFSPAFSRPSAFSSLAESDPGPPRASLRAKTSPEGARDLLGPKALPGSSQ	191		
Sbjct 127	-----	QHIGCGYNNA-ARP--FSNGGDG-----GVKSIVN-----	153		
Query 192	PROYNN	PIGLYSAETLREMAQMYQMSLRGKASGVGL	227		
Sbjct 154	-KQYN	TPVGIYSDESIAETLSAQAEVLAGGVLGVNF	188		

Figure 4: Results of the alignment between human Zasp (query) and *Drosophila* Zasp52 (subject) using NCBI BlastP. The alignment identified five conserved regions; this figure highlights range 2 (amino acids 18–188). Conserved residues are indicated as follows: A147 (yellow arrow), V55 (green arrow), and R16 (blue arrow), all of which are well-conserved between the two systems.

In addition to the point mutations reported by Sheikh *et al.* (2007), over 500 allelic variants of unknown significance are listed in the ClinVar database. Each of these variants could be individually analyzed using the same methodology described in this section to determine whether the mutation falls within conserved amino acid regions. To prioritize the most promising mutations, the following criteria will be applied: the mutation must be a single nucleotide variant; it must be associated with a potential condition, such as myofibrillar myopathy or dilated cardiomyopathy; and it must have a review status of at least two stars in ClinVar (indicating corroboration by more than one record). Once these criteria are met, the mutation's conservation across species must be confirmed through sequence alignment. An example is the R16H mutation, identified as a promising variant in

ClinVar (Figure 5) and shown to be identical between human *Zasp* and *Drosophila* Zasp52 (Figure 4, blue arrow). In Figure 5 examples of these mutations are shown, an exhaustive bioinformatic analysis has to be done to know exactly how many out of the 570 results do follow this criteria.



Search results

Display options ▾ Sort by Location ▾ Download ▾

Items: 1 to 100 of 570

Filters activated: Uncertain significance, At least one star. [Clear all](#) to show 1018 items.

Variation	Gene (Protein Change)	Type (Consequence)	Condition	Classification, Review status
<input type="checkbox"/> NM_007078.3(LDB3):c.46C>T (p.Arg16Cys)	LDB3 (R16C)	Single nucleotide variant (missense variant)	Myofibrillar myopathy 4	Uncertain significance ★
<input type="checkbox"/> NM_007078.3(LDB3):c.47G>A (p.Arg16His)	LDB3 (R16H)	Single nucleotide variant (missense variant)	Myofibrillar myopathy 4 +1 more	Uncertain significance ★★
<input type="checkbox"/> NM_007078.3(LDB3):c.54G>T (p.Gln18His)	LDB3 (Q18H)	Single nucleotide variant (missense variant)	Dilated cardiomyopathy 1C +4 more	Uncertain significance ★★
<input type="checkbox"/> NM_007078.3(LDB3):c.55G>C (p.Gly19Arg)	LDB3 (G19R)	Single nucleotide variant (missense variant)	Cardiovascular phenotype +2 more	Uncertain significance ★★
<input type="checkbox"/> NM_007078.3(LDB3):c.55G>A (p.Gly19Arg)	LDB3 (G19R)	Single nucleotide variant (missense variant)	not provided +1 more	Uncertain significance ★★
<input type="checkbox"/> NM_007078.3(LDB3):c.55G>T (p.Gly19Trp)	LDB3 (G19W)	Single nucleotide variant (missense variant)	Myofibrillar myopathy 4 +1 more	Uncertain significance ★★
<input type="checkbox"/> NM_007078.3(LDB3):c.56G>C (p.Gly19Ala)	LDB3 (G19A)	Single nucleotide variant (missense variant)	Myofibrillar myopathy 4 +1 more	Uncertain significance ★★

Figure 5: Example of reported clinical variants of human Zasp in ClinVar. Of the 570 reported variants, here 7 that meet the research criteria and are well-conserved are shown. The R16H variant is indicated by a blue arrow.

Bioinformatic design for Zasp52-PR-607P>L.

The UniProt amino acid sequence "O75112" (LDB3_HUMAN) and the FlyBase amino acid sequence "Dmel\Zasp52-RR" were downloaded. Both sequences were aligned using the BlastP NCBI tool, and the proline was confirmed

to be in a homologous position 608 (human) and 607 (*Drosophila*). After Proline 607 was identified, Zasp52-RR was reverse-translated using ExPasy, and this analysis showed that this proline was encoded by the nucleotide sequence "CCC." To emulate the human point mutation 608P>L, the nucleotide sequence was changed to "CTC," which encodes leucine. The plasmid "pUASTattB," a common vector for expressing transgenes under UAS, was chosen for fly cloning. The NebCutter online tool was used to select restriction sites compatible with the sequence to be cloned, avoid repeated restriction sites within the sequence, and determine the expression direction. "EcoRI" (restriction site: GAATTC) and "NotI" (restriction site: GGCCGC) were the enzymes chosen. The Flag-strep-his-tag was added to simplify purification. The final sequence for Zasp52-PR-607P>L is shown below:

```
GAATTCATGGACTACAAAGACCATGACGGTGATTATAAAGATCATGACATCGAC
TACAAGGATGACGATGACAAGGAGAACCTGTACTTCCAGTCCAACCTGGAGCCA
CCCGCAGTTTCGAAAAGCATCACCATCACCATCACGCCCAACCACAGCTGCTG
CAAATCAAATTGTCACGTTTCGATGCCCAACCCTGGGGATTCCGCCTTCAGGG
GGGCACGGACTTCGCTCAGCCCCTGCTGGTGCAAAAGGTGAACGCCGGCAG
CTTGTCCGAGCAGGCTGGCCTCCAGCCCGGCGATGCGGTGGTCAAGATCAAT
GACGTGGATGTCTTCAATCTGCGTCACAAGGATGCCCAGGACATTGTGGTGC
GCTCCGGCAACAACCTTTGTCATCACAGTGACGCGCGGTGGCTCCACCTGGCG
CCCGCATGTGACACCGACTGGCAATGTGCCGCAGCCCAACTCGCCGTATCTG
CAGACGGTGACGAAGACCTCTCTGGCTCACAACAACAGGACAGCCAGCACA
TCGGCTGTGGCTACAACAACGCGGCCCGTCCCTTCTCCAACGGCGGCGATG
GCGGCGTGAAGAGCATTGTCAATAACAATAACAACACCCCGGTTGGCATTAC
AGCGATGAATCTATTGCGGAAACACTCTCGGCCCAGGCGGAGGTTTTGGCTG
GCGGTGTGCTCGGCGTCAACTTCAAGAAGAACGAGAAGGAATACCAGGGCGA
TCGCTCCGAGGTTCTGAAGTTCCTGCGCGAGGAGGAGACCGGCCAGTCCAC
TCCAGCATTTCGGCAATAGCCACTACGAGCATGATGCACCACAGCAACTGCAAC
AGCCACAACAGCAATACAACCAACACCAGCAACACTATCACCAGCAACAACAA
CAACAGCAATCGAGCACCCTCGCCATGTCAGCGCCCCCGTGAACCTCCCCCA
AGCCCCCGAGCACCGGCGGACTCCCAACTGGCCAGAACATTTGCACCGAATG
CGAGCGCCTCATTACTGGCGTTTTTCGTGCGCATCAAGGATAAGAACCTGCACG
TGGAGTGCTTCAAGTGTGCCACGTGTGGCACCTCGCTGAAGAACCAGGGGCTA
CTACAACCTTCAACAACAAGCTCTACTGCGACATCCACGCCAAACAGGCCGCCA
```

TCAACAATCCCCCACCAGGACCGAGGGCTACGTCCCCGTTCCCATCAAGCC
CAACACCAAGCTGAGTGCCTCCACCATCTCATCGGCCTTGAAGCTGCACGGAT
ACGGTGGCCACTCGAACGGCTACTCCAATGGAACTCCACCCCTGCTCCGGC
ACCGGTGAACCAGGGCTATGCTCGTCCGTTCCGGTGCCGCCGCTCCCAAGTCG
CCGGTGTCTATCCGCCGCAGCAGCAACAGCAGTCGCCGCGTCCCGCTCCC
GGTGGCCAAAACCCGTACGCCACCCTGCCCCGCAGCAATGTGGGGCCAACAA
GGTCGTAATGTAAGGTACCAACAACAGCAACAACAGCAGCAGCAATACAACAA
TCAGCAGAAGCAGCAGTATAGGAACTCTTACCCCATGGGATCTAATTATAGCAC
CCCGAGTCAGTCCCCCTACATCACCTCCAACACCAACAACACTATAGCAGCAGCA
ACAGCTACAATAACAACAACACTATAGCAACTACAACAATAATAATGTGTACCGAGG
TGCCGGAGGAAAGAGCGCTGGCGCCTTTGGAGCCACCTCGGCGCCCAAGAG
GGGCAGGGGTATCCTGAATAAGGCAGCCGGACCCGGAGTGCGCATCCCACT
GTGCAACAGCTGCAATGTGCAGATCAGAGGACCCTTTATCACGGCATTGGGCC
GCATCTGGTGCCCGGATCATTTTCATCTGCGTGAACGGCAACTGCCGTCGTCC
GCTGCAGGACATTGGATTGTTGAGGAGAAGGGCGATCTGTACTGCGAGTAC
TGTTTCGAGAAGTACCTGGCGCTC ACTTGCAGCAAGTGCGCTGGCAAGATCA
AGGGTGACTGTTTGAATGCCATTGGCAAACACTTCCATCCGGAGTGCTTCACC
TGCGGCCAGTGCGGCAAGATCTTTGGCAACAGGCCCTTCTTCTGGAGGATG
GAAACGCGTACTGCGAGGCCGATTGGAACGAGTTGTTACCAACCAAGTGCTT
CGCCTGCGGCTTCCCCGTGGAAGCTGGCGACAGATGGGTGGAGGCCTTGAA
CCACAACACTACCATAGCCAATGCTTCAACTGCACGTTCTGCAAACAGAACCTGG
AGGGTCAGAGCTTCTACAACAAGGGCGGACGTCCCTTCTGCAAGAATCACGC
GCGCTAATAGCGCGCCGC

Color Code:

Start Codon

Stop Codon

EcoRI restriction site.

NotI restriction site

Flag-strep-his-tag

607P>L Mutation

This final sequence was sent to Genscript for the “607P>L-Zasp52” genotype.

Fly stocks and genetics.

Standard genetic crosses were performed to obtain the Zasp52 null mutant. The Zasp52 5’3’ FRT (designed by CRISPR)/CyO stock was crossed with Hs-Flp; Sp/CyO. This initial cross was incubated for three days at 28°C, after which the

adult flies were transferred to fresh food to start the heat shocks on the offspring. On the third day after the initial cross, the first heat shock was conducted at 37°C for one hour, and this process was repeated twice more, 24 hours after the previous heat shock. When the flies reached adulthood, female flies were selected against the Sp marker for a second standard genetic cross with the Tft/CyO stock. The offspring males were selected against Tft and analyzed for the absence of fluorescence (GFP and RFP). The males with no fluorescence after the second genetic cross were heterozygous for the Zasp52 null mutation, and these males were crossed again with Tft/CyO. The offspring of the third cross were selected against Tft, and both females and males were chosen to establish a Zasp52 null homozygous stock through a fourth genetic cross.

Standard genetic crosses were performed to obtain the Zasp52-Zasp66 and Zasp52-Zasp67 double null mutants, as well as the Zasp52-Zasp66-Zasp67 triple null mutant. The following fly stocks were used: Zasp66-Zasp67 double null / TM3-Sb (González-Morales *et al.*, 2019), Sp/CTG; Dr/TTG, Zasp67 null (González-Morales *et al.*, 2019), and Zasp66/TM6B (González-Morales *et al.*, 2019).

For the overexpression assays, the Act88F-Gal4 (Bryantsev *et al.*, 2021) fly stock was crossed with Zasp52-PR/Tm3-Sb, Zasp52-PR-607P>L/Tm3-Sb, and Human-Zasp-l2. The crosses were maintained at 18°C to limit overexpression.

For the rescue assays, these different UAS-transgenes (Zasp52-PR, Zasp52-PR-607P>L, and Human-Zasp-I2) were expressed in a Zasp52 homozygous null mutant background under the Act88F-Gal4 driver.

Western analysis:

The western blot protocol was consistent for all samples: three fly thoraces were homogenized in 2x SDS sample buffer, followed by protein sample separation using 8% SDS-PAGE. The Zasp52 null deletion was preliminarily confirmed by immunoblotting with a rabbit Zasp-FL antibody (Jani and Schöck, 2007). Immunoblotting with anti-FLAG (1:5000, Sigma-Aldrich) was used to confirm the overexpression of the transgenes: Human-ZaspI2, Zasp52-PR, and Zasp52-PR-anti-607P>L.

Determination of death stage.

An embryo collection was conducted to determine the stage of death for the Zasp52-Zasp66-Zasp67 triple null mutant and the Zasp52-Zasp66 double null mutant, using a culture medium composed of agarose (3.5%), sucrose (3.5%), and apple juice (35%). The embryo collection lasted four hours, after which adult flies were transferred to fresh food, and the embryos were incubated at 28°C for 20 hours. Both stocks contained double balancers: "CTG" (Curly, GFP) and "TTG" (Tm3, GFP). To select homozygous mutants, all GFP embryos were discarded; the remaining embryos were counted and incubated at 28°C. The culture was analyzed every 24 hours after selection, and survivors were counted.

PCR.

DNA extraction.

The DNA extraction protocol was followed as described by QIAGEN in their “Purification of Total DNA from Insects Using the DNeasy® Blood & Tissue Kit.”.

PCR primers.

Primers were designed using Benchling to verify the deletion of the *Drosophila* Zasp genes (Zasp52, Zasp66, and Zasp67). Gene sequences were obtained from Flybase, with Zasp52 identified as FBgn0265991, Zasp66 as FBgn0035917, and Zasp67 as FBgn0036044. For positive control, primers were designed for a small genetic construct available in the lab, the “Zasp52-PR” plasmid, Flybase ID: FBpp0302946.

- Zasp52
 - FWD: 5' TTTAGGTGTCTCGCTTGGTG 3'.
 - REV: 5' TGTGCGTTTTGGGCGTT 3'.
- Zasp66
 - FWD: 5' ACAAATCGCCTACACGCA 3' . ,
 - REV: 5' CGATGGAACCTTGACCAAC 3'.
- Zasp67
 - FWD: 5' TTCCCTCCTTGACTACTTCCC 3'.
 - REV: 5' GGTGTTGATGGTGTGGTG 3'.
- Plasmid 52 PR LINE
 - FWD: 5' TGCTGGTGCAAAGGTGA 3'

- REV: 5' TAGTAGCCCTGGTTCTTCAG 3'

Figures 6, 7, 8, and 9 depict the predicted PCR product for each gene (indicated by the green arrow). In addition to the expected product size, the figures display other critical properties of the designed primers for the PCR assay, including their 3' location in the sequence, melting temperature (T_m), GC content, and primer length.



	5' TTTAGGTGTCTCGCTTGGTG 3'	5' TGTGCGTTTGGGCGTT 3'
3' Location	32226	33194
T _m 	59.1°C	59.6°C
GC Content	50.00%	52.94%
Length	20 bp	17 bp
<hr/>		
Product Size	1004 bp	

Figure 6: Predicted primer properties and expected PCR result for amplification of Zasp52 gene, product size expected of 1004 bp.

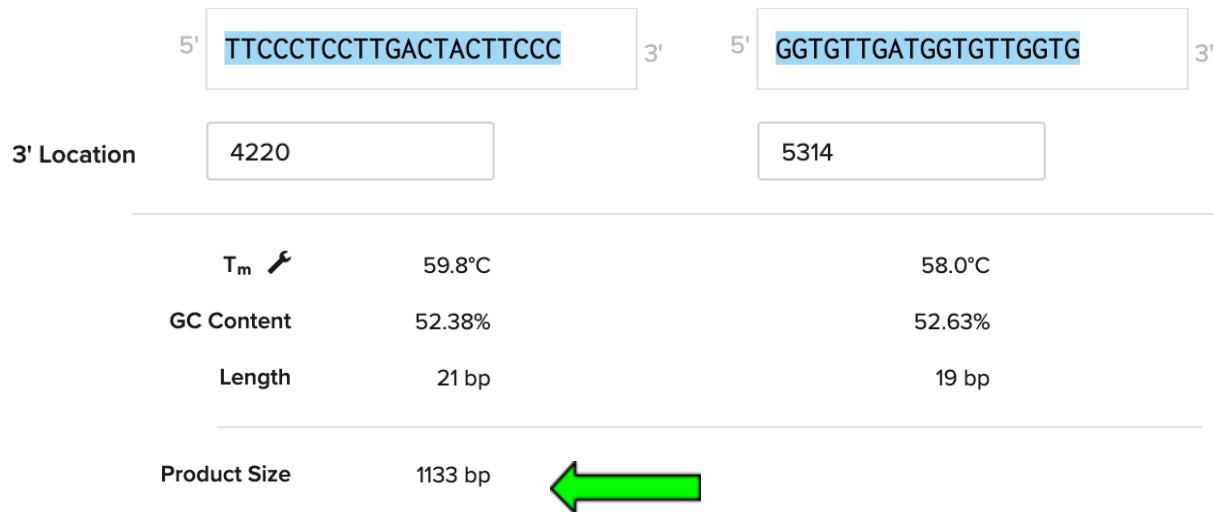


Figure 7: Predicted primer properties and expected PCR result for amplification of Zasp67 gene, product size expected of 1133 pb.

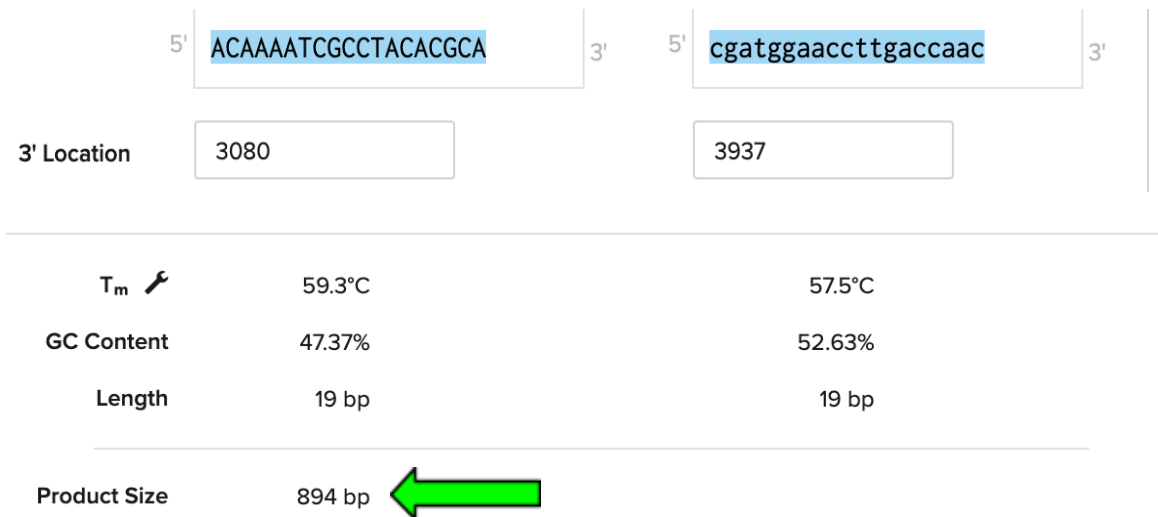


Figure 8: Predicted primer properties and expected PCR result for amplification of Zasp66 gene, product size expected of 894 pb.

5'	TGCTGGTGCAAAGGTGA	3'	5'	TAGTAGCCCTGGTTCTTCAG	3'
----	-------------------	----	----	----------------------	----

T_m 	58.6°C	57.2°C
GC Content	50.00%	50.00%
Length	18 bp	20 bp
<hr/>		
Product Size	979 bp	

Figure 9: Predicted primer properties and expected PCR result for amplification of Zasp52-PR plasmid, product size expected of 979 pb.

PCR conditions:

The reaction mixture composition was followed as described by “Thermo Scientific Phire Plant Direct PCR Kit”. The company suggests mixture compositions in their protocol to have a final solution of 20 μ L:

- 10 μ L of the 2X Phire Plant PCR Buffer.
- 0.4 μ L Phire Hot Start II DNA Polymerase.
- Primer FWD. 1 μ L (final concentration of 0.5 μ M)
- Primer REV: 1 μ L (final concentration of 0.5 μ M)
- DNA: 3 μ L (final concentration of 0.5 μ M)
- DMSO: 0.6 μ L
- H₂O: 4 μ L

For thermocycling conditions:(Biometra Thermocycler TProfessional Basic 96 gradient)

- Initial denaturation: 94°C for 3 minutes.
- Cycling Conditions:
 - Denaturation: 94°C for 5 seconds
 - Annealing: The Ta was different for each set of primers. Zasp52: 57°C, Zasp66: 61.5°C, Zasp67: 62°C, and for the plasmid: 61.5°C. All of the PCR assays have a Ta time of 5 seconds.
 - Extension: 72°C for 15 seconds
- Number of Cycles: 15
- Final Extension: 72°C for 5 minutes.

DNA gel was prepared for PCR product revelation, agarose 1% diluted in a buffer solution containing a mixture of Tris base, acetic acid, and EDTA (TAE). For gel revelation, SYBR™ Safe DNA Gel Stain was added to get a final concentration of 0.1 µl/mL of agarose gel. The Electrophoresis chamber used was MYGEL Mini electrophoresis system from scientific laboratory supplies.

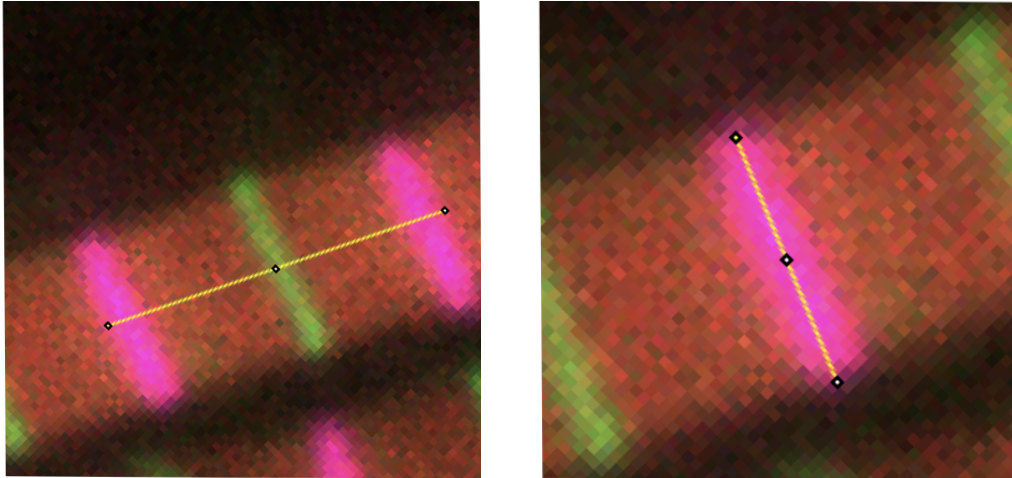
Immunofluorescent staining and confocal microscopy.

For immunofluorescent staining of IFMs, the following primary antibodies were used: rat anti-sls (kettin), Alexa 594-Phalloidin, and rabbit anti-obscurin Ig 14-16 (Katzemich *et al.*, 2012). The secondary antibodies used were anti-rat-647 and anti-rabbit-488. The described protocol was applied to the following stocks: Zasp52 null, Zasp52-Zasp67 double null, Act88F-Gal4-UAS-607P>L, Zasp52PR, and Act88F-Gal4-UAS-Zasp52PR.

Twenty-half thoraces were glycerinated in YMG (20 mM Na-Phosphate, 2 mM MgCl_2 , 2 mM EGTA, 5 mM DTT, 0.5% Triton X-100, 50% glycerol) overnight at -20°C . IFMs were dissected by removing the cuticle and extracting the myofibrils, which were then washed three times with a relaxing solution (20 mM Na-Phosphate, 5 mM MgCl_2 , 5 mM EGTA, 5 mM DTT, 5 mM ATP, protease inhibitor, pH 7.2). Myofibrils were fixed with 200 μL of 4% paraformaldehyde (prepared by diluting 8% PFA with the relaxing solution) for 10 minutes at room temperature. The fixation solution was removed, and the samples were washed three additional times with the relaxing solution. Primary antibody incubation was performed overnight (1:400 dilution in relaxing solution). The following day, samples were washed three times with the relaxing solution, then incubated with Alexa 594-Phalloidin and secondary antibodies (1:200 dilution in relaxing solution) for 2 hours. Samples were mounted in ProLong Gold antifade solution (Life Technologies, Ontario, Canada). Images were acquired using a Leica CIAN-SP8 Confocal Laser Scanning Microscope with an HC PL APO 63x/1.40 OIL CS2 oil immersion objective.

Quantifications.

Quantifications were performed using Fiji: ImageJ, focusing on two main measurements: sarcomere length and sarcomere width, as shown in Figures 10 and 11, respectively.



Figures 10 and 11: Sarcomere length and width quantifications using Fiji: ImageJ. Actin filaments are shown in red, Z-discs in purple, and M-lines in green. Sarcomere length (Figure 10) is defined as the horizontal distance between the bordering Z-discs of the sarcomere. Sarcomere width (Figure 11) is the vertical distance across the Z-disc, representing the myofibril diameter.

Electron microscopy

Thoraces were dissected in dissection buffer (100 mM sucrose, 100 mM Na phosphate, pH 7.2, 2 mM EGTA) and subjected to overnight primary fixation in dissection buffer containing primary fixatives (3% paraformaldehyde, 2%

glutaraldehyde) at 4°C. Samples were then washed in dissection buffer and secondary fixed in 100 mM phosphate buffer with 1% OsO₄. Dehydration was performed through an ethanol series of 25%, 50%, 70%, 90%, and 100%, with samples left in 100% ethanol overnight. The following day, samples were washed with epoxypropane, and the Epon mix was prepared as follows: 46% Epon 815, 28% DDSA, 24% NMA, and 2% DMP30. For resin infiltration, samples were treated with 25%, 50%, and 100% Epon mix diluted in epoxypropane. Thoraces were oriented in BEEM capsules and filled with the Epon mix. Images were obtained using FEI Tecnai G2 Spirit BioTwin 120 kV Cryo-TEM.

Yeast two-hybrid assay.

Plasmid construction.

Former Schöck Lab student Marie-Pier Lalonde designed the plasmids. Nucleotide sequences corresponding to LIM2b + LIM3 and LIM2b + LIM3 + LIM4, LIM2b+ LIM3-607P>L, LIM2b + LIM3 + LIM4-607P>L including the linker sequences between the protein domains, were cloned by Genscript into the pGBKT7 BD yeast expression vector (Takara Bio). These prey vectors contained a kanamycin resistance gene for selection in *E. coli* and tryptophan (W) nutritional marker for selection in yeast. The restriction site EcoRI (G>AATTC) was added at the beginning of the insert sequence, located at position 1299 on the pGBKT7 plasmid. The Sall restriction site (G>TCGAC) was added at the end of the insert sequence, corresponding to position 1315 on the plasmid. These sites were within the multiple cloning site and in frame with the Gal4 DNA binding domain. The bait

vector consisted of the Zasp66-PK sequence cloned into the pGADT7 AD plasmid (Takara Bio), creating fusion proteins with the Gal4 activating domain, ampicillin resistance gene, and leucine (L) marker.

Bacterial transformation, and mini-prep.

To amplify the plasmid constructs, they were transformed into *E. coli* and purified. Competent bacterial cells were incubated with mercaptoethanol for 10 minutes and with the appropriate plasmid DNA for 30 minutes on ice, then heat shocked at 42°C for 30 seconds. Successfully transformed *E. coli* cells were selected by growth on kanamycin or ampicillin plates. Liquid cultures were inoculated with a single transformed colony and grown overnight, shaking at 37°C. Plasmid DNA was purified according to the protocol of the EZ-10 Spin Column handbook (BioBasic). After lysis and neutralization, plasmid DNA was selectively adsorbed in a silica gel-based column, and impurities were washed away. The plasmid DNA was then eluted and stored at -20°C.

Yeast 2 Hybrid assay

LIM protein plasmids (wildtype and mutant) were co-transformed with the Zasp66 plasmid in Y2H Gold competent yeast cells according to the Yeastmaker Yeast Transformation standard small-scale protocol (Takara Bio). As a control, the LIM protein constructs were also co-transformed with the empty pGAD plasmid, and vice versa, the Zasp66 plasmid was co-transformed with the empty pGBK plasmid. The yeast cells were grown overnight in a YPDA liquid medium and then washed three times with water. After the first wash with 1.1X TE/LiAc solution, the

yeast cells were resuspended in 1.1X TE/LiAc (50 μ L). Then, 100 ng of plasmid DNA was mixed with 5 μ L denatured Yeastmaker Carrier DNA (salmon sperm DNA, 10 μ g/ μ L), 50 μ L competent yeast cells, and 500 μ L PEG/LiAc solution before being incubated while shaking for 30 minutes at 30°C. 20 μ L of DMSO was added before the cells were heat shocked at 42°C for 15 minutes. After the transformation, the cells were pelleted and resuspended in 1 mL YPD Plus Medium, incubated while shaking at 30°C for 90 minutes, and then washed and resuspended in 100 μ L of water. Successful transformations were evaluated by growth on -WL (tryptophan and leucine) nutrition drop-out plates. Five days later, these colonies were resuspended in 100 μ L of water and dropped onto -WLH (tryptophan, leucine, histidine) and -WLHA (tryptophan, leucine, histidine, and adenine) drop-out plates. A 1/5 serial dilution in water was also performed on -WLHA plates. For the mutant LIM transformations, the cells were dropped on -WLH and -WLHA plates containing two concentrations of 3-AT (5 mM and 7.5 mM).

Yeast mating

LIM2b3, LIM2b34, LIM2b3607P>L, and LIM2b34607P>L protein plasmids were individually transformed into Y2H Gold competent yeast cells. The Zasp66 plasmid and empty pGADT7 plasmid were also individually transformed into Y187 competent yeast cells. Both transformations were performed according to the Yeastmaker Yeast Transformation standard small-scale protocol (Takara Bio) and followed the same procedures as the co-transformations described above. The LIM-pGBK-transformed Y2H Gold yeast was plated on -Leucine plates to select

successful transformants. The Z66-pGAD and empty pGAD-transformed Y187 yeast were plated on -Tryptophan plates to select successful transformants. Both strains were then mated by streaking one on top of the other on -WL plates. The Y2H Gold yeast genotype was MATa, and the Y187 genotype was MATalpha. The mating strategy differed from the previous Y2H in that two haploid yeast strains that independently expressed the bait and prey fusion plasmids were combined. Diploid growth was observed on the -WL plates. Finally, the diploid yeast was streaked out on -WLH and -WLHA plates to verify protein interactions by reporter biosynthetic gene activation.

Results:

General aim 1: Design and analyze Zasp null mutants.

Design of Zasp52 null mutant: Flightless mutants and the absence of GFP and RFP preliminary confirms Zasp52 complete gene deletion.

The main complication in designing the Zasp52 null mutant was its large locus with numerous splice variants. To entirely delete the *Drosophila* Zasp52 gene, the Schöck Lab utilized a two-step CRISPR approach, first targeting the PDZ domain and then LIM domain 4 (Figure 12). Following these deletions, homology-directed repair enabled the insertion of FRT sites and fluorescent markers (C-terminal RFP and N-terminal GFP) at the deletion sites. These FRT sites flanked a 20 kb region that includes the remaining functional domains of

Zasp52, as shown in Figure 12. Genetic crosses described in the Materials and Methods were followed, and the deletion was verified by an absence of GFP and RFP markers under fluorescence microscopy, establishing a homozygous Zasp52 null mutant stock. This novel *Drosophila* Zasp52 null mutant was viable but displayed complete flightlessness.

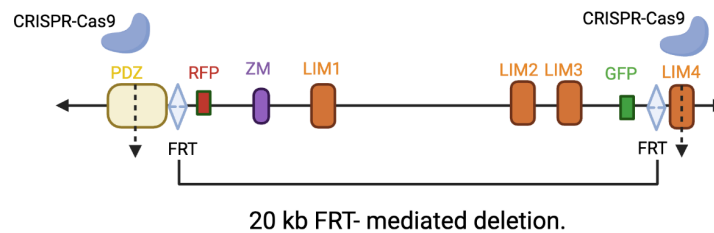


Figure 12: Zasp52 null mutant design. A cartoon made on Biorender of the Zasp52 genomic locus is shown, describing the extent of the N-GFP-FRT and C-FRT-RFP CRISPR mutation for the Zasp52 null mutant.

Confirmation of Zasp52 null mutant: Western blot incubated with Zasp52 full-length antibody does not detect any isoforms in a *Drosophila* Zasp52 null mutant.

To confirm the deletion of Zasp52 at the molecular level, a Western blot was performed using the Zasp-Full-length antibody previously designed by the Schöck Lab (Jani and Schöck, 2007), which targets an antigen significantly overlapping with all predicted Zasp52 isoforms (Katzemich *et al.*, 2011). Two wild-type samples were positive controls (Figure 13, B, and E). The antibody detected at least three isoforms in the wild-type samples (Figures 13, B, and E), based on the bioinformatic tool “protein molecular weight”, Zasp52-PR one of the main isoforms

should have around 80 kDa (Pointed out in Figure 13). However, no bands were detected in the triplicate of Zasp52 null mutant samples, as indicated by the lack of antibody binding (Figure 13, B, and E). This result serves as the first molecular confirmation of the Zasp52 null mutant.

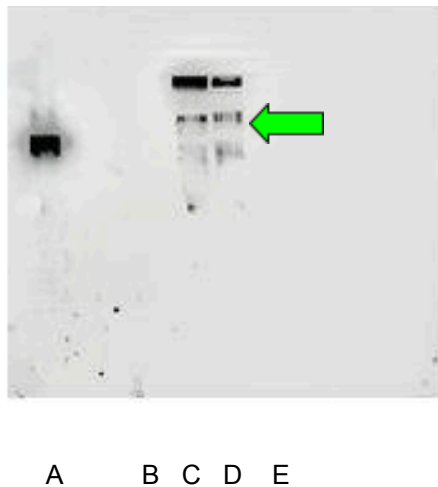


Figure 13: Western blot incubated with Zasp52 full-length antibody does not detect any isoforms in a *Drosophila* Zasp52 null mutant. Lane A displays the protein ladder marked at 75 kDa, made visible using the western blot marker pen. Lanes B and E contained protein samples from Zasp52 null homozygous mutants. Lanes C and D contained wild-type protein samples. The green arrow points out bands of approximately 80 kDa.

Confirmation of Zasp52 null mutant: Zasp52-designed primers amplify the Zasp52 gene in a wild-type sample, but no product is detected in the Zasp52 null mutant.

To confirm the deletion of the Zasp52 gene in the null mutants, a PCR assay was performed with primers specifically designed to amplify the three *Drosophila* Zasp genes: Zasp52, Zasp66, and Zasp67. Wild-type DNA samples and a Zasp52-PR plasmid construct were used as positive controls to ensure the PCR conditions were optimal.

Figures 14 and 15 display the amplification results for wild-type DNA and the Zasp52-PR plasmid under these optimized conditions. In Figure 14, the Zasp52 gene is successfully amplified in a wild-type sample, with a band at the expected size of 1004 bp, slightly larger than the 979 bp band of the Zasp52-PR plasmid construct. Figure 15 shows the successful amplification of Zasp66 (894 bp) and Zasp67 (1133 bp) in wild-type samples, as indicated by the green arrow marking the 1000 bp molecular size marker.

In Figure 16, the PCR assay results for the Zasp52 null mutant DNA show the absence of Zasp52 amplification in Lane B, indicating successful gene deletion. In contrast, Lanes C and D confirm the presence of Zasp66 and Zasp67 in the null mutant DNA samples, as the expected bands are observed for both genes.

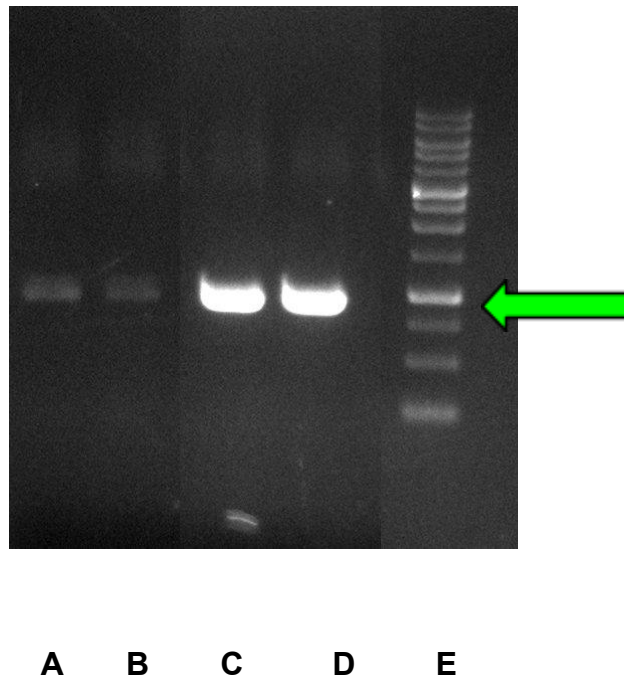


Figure 14: PCR assay confirms the amplification of the Zasp52 full-length gene in a wild-type sample. The molecular weight ladder is labeled as "G," with the arrow indicating the 1000 bp molecular size. Lanes A and B contained wild-type DNA samples incubated with Zasp52 primers. Lanes C and D contained Zasp52-PR DNA plasmid samples incubated with plasmid-specific primers.

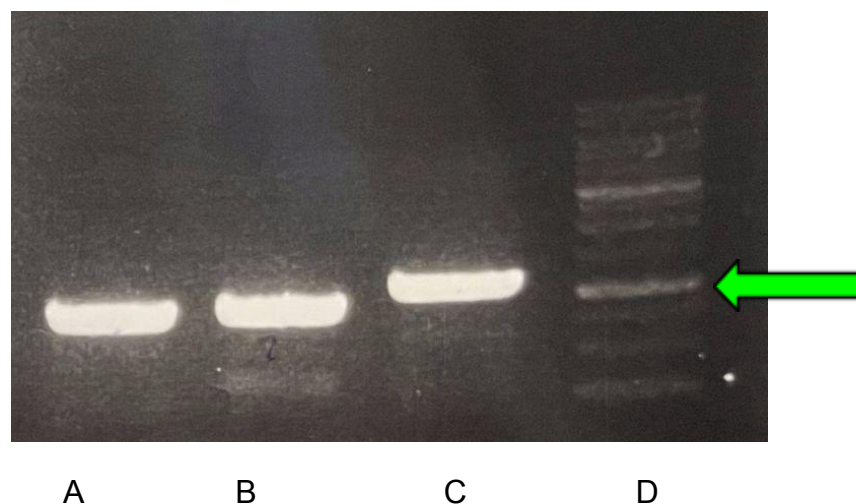


Figure 15: PCR assay confirms the amplification of Zasp66 and Zasp67b in a wild-type sample. The molecular weight ladder is labeled as "D," with the arrow indicating the 1000 bp molecular size. Lane A contained Zasp52-PR DNA plasmid samples incubated with plasmid-specific primers. Lane B contained wild-type DNA samples incubated with Zasp66 primers. Lane C contained wild-type DNA samples incubated with Zasp67 primers.

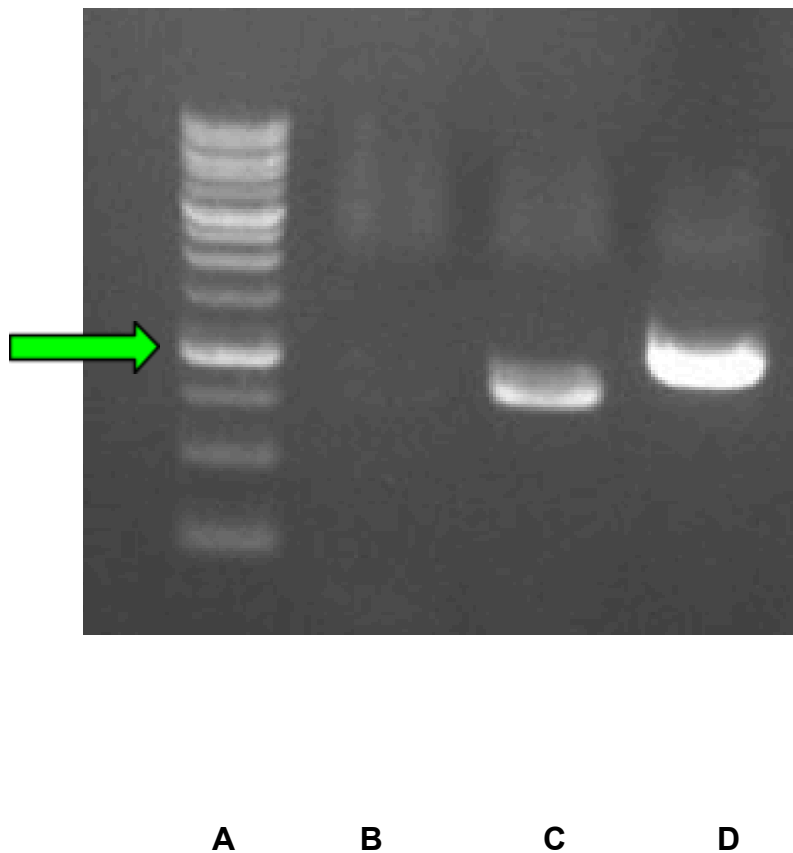


Figure 16: PCR assay confirms the Zasp52 null mutant. The molecular weight ladder is labeled as "A," with the arrow indicating the 1000 bp molecular size, this PCR assay was incubated with Zasp52 DNA null mutant samples (Lanes B, C, and

D). Each lane was incubated with pair primers for the different genes. Lane B: Zasp52, Lane C: Zasp66, Lane D: Zasp67.

Confirmation of the Zasp52-Zasp67 double null mutant: Zasp67-designed primers amplify the Zasp67 gene in a wild-type sample, but no product is detected in the Zasp52-Zasp67 double null mutant.

Similar to the confirmation of the Zasp52 null mutant, in Figure 17 a PCR assay confirming the deletion of Zasp52, and Zasp67 is shown. Lane A still shows the amplification of Zasp66, but the absence of product in lanes B, and C shows the deletion of Zasp67 and Zasp52 genes respectively.

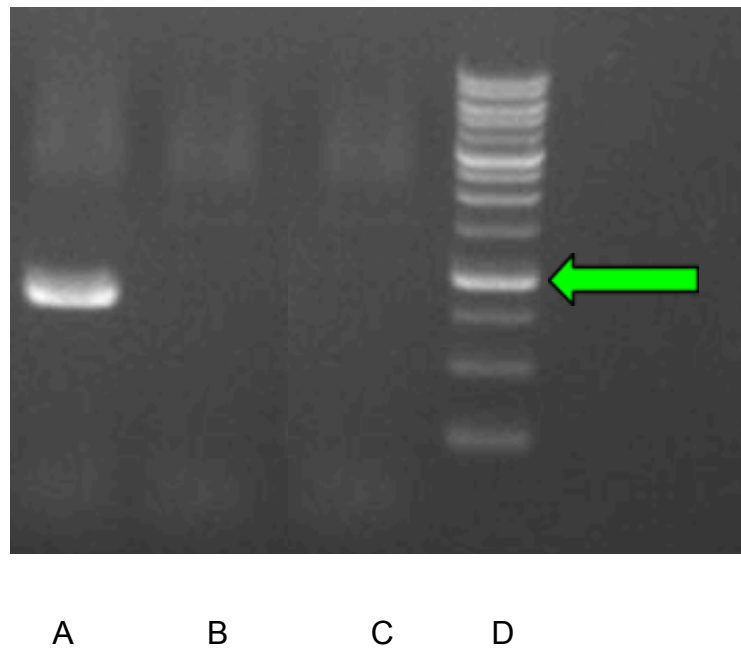


Figure 17: The PCR assay confirms the Zasp52-Zasp67 double null mutant.

The molecular weight ladder is labeled as "D," with the arrow indicating the 1000 bp molecular size. This PCR assay was incubated with Zasp52-Zasp67 double null

mutant DNA samples (Lanes A, B, and C). Each lane was incubated with pair primers for the different genes. Lane A: Zasp66, Lane B: Zasp67, Lane C: Zasp52.

Analysis of Zasp null mutants: Confocal microscopy of Zasp null mutants reveals severe IFM defects.

The muscle phenotype of the IFMs in Zasp52 and Zasp52-Zasp67 null mutants was assessed through confocal microscopy. In the Zasp52 null mutant, myofibrils were observed to be frayed and ruptured (Figure 18-A). The Zasp52-Zasp67 double null mutant exacerbated the phenotype, with the myofibril components losing any organized structure (Figure 18-B). Despite these structural defects, the Zasp52 null and Zasp52-67 double null mutants were viable but entirely flightless.

Additionally, in the wild-type IFMs, myofibrils displayed an ordered structure, consistent diameter, and regular sarcomere markers (Figure 18-A). In contrast, the Zasp52 null mutant showed wavy myofibrils with irregular Z-discs, M-lines of varying sizes, and inconsistent sarcomere spacing (Figure 18-B, yellow arrow). Myofibril disruption was very severe in the Zasp52-Zasp67 double null mutant, as indicated by the yellow arrow in Figure 18-C.

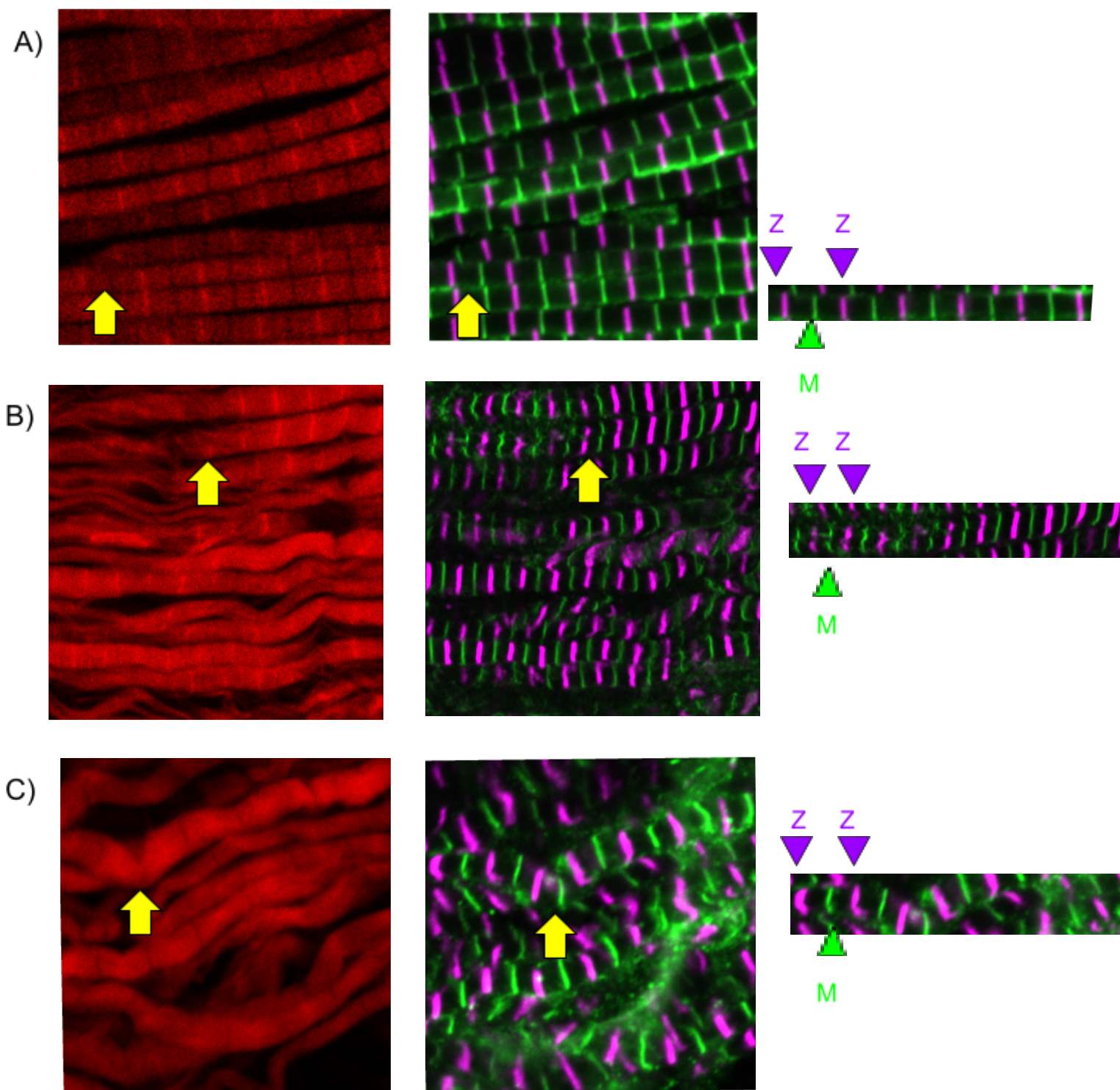


Figure 18: Confocal microscopy of the Zasp52 null mutant revealed severe defects in the indirect flight muscles (IFMs), which were further exacerbated in the

Zasp52-67 double null mutant. Confocal images of 5-day-old flies IFM's from different genotypes. Actin filaments are stained with phalloidin (red), anti-SIs were used to mark the Z-discs (magenta), and anti-obscurin ig 14-16 was used to mark the M-lines. **A)** Wild-type control flies have a stereotypic sarcomere organization. **B)** Zasp52 null mutant IFMs showing broken and disorganized. **C)** Zasp52-67 double null mutant IFMs showing a worsened phenotype. For each sample, a single myofibril is indicated with a yellow arrow, and on the far right, a sarcomere is highlighted with two Z-discs (magenta) and one M-line (green).

Quantifications of sarcomere length and sarcomere width reveal aberrant myofibril sizes in Zasp52 null mutants and Zasp52-67 double null mutants.

Using PRISM, sarcomere length, and width measurements were obtained for wild-type and null mutant muscles to quantify the muscle phenotypes. For each phenotype, triplicate immunostainings were conducted, and 50 measurements per sarcomere dimension were taken, resulting in 150 measurements per each phenotype sarcomere dimension. The analysis included at least 15 different genotypes per *Drosophila* stock, and T-tests were performed to compare the means between samples. Significance was indicated by P-values, represented by asterisks, with categories as follows: **** (extremely strong evidence), *** (very strong evidence), ** (good evidence), * (moderate evidence), and ns (no significant difference).

The median sarcomere length in wild-type samples was 3.24 microns (Figure 19-A), consistent with the literature value of approximately 3.2 microns

(Spletter *et al.*, 2018). The sarcomere lengths of the Zasp52 and Zasp52-Zasp67 null mutants were shorter than the wild type, with greater data dispersion observed in the double null mutant. T-tests yielded $P < 0.0001$ for comparisons between wild-type and Zasp52 null mutants and wild-type and Zasp52-Zasp67 double null mutants, indicating extremely significant differences in both cases.

For sarcomere width (Figure 19-B), the wild-type median was 1.43 microns, closely aligning with the reported 1.5 microns (Schöck and Gonzáles, 2022). While the wild-type sample showed clustering around the median, the null mutants displayed more variation. The double null mutant's mean sarcomere width was smaller than the wild type at 1.01 microns, whereas the Zasp52 null mutant had a larger mean width of 1.67 microns. Both comparisons with the wild type also yielded $P < 0.0001$, confirming extremely significant differences.

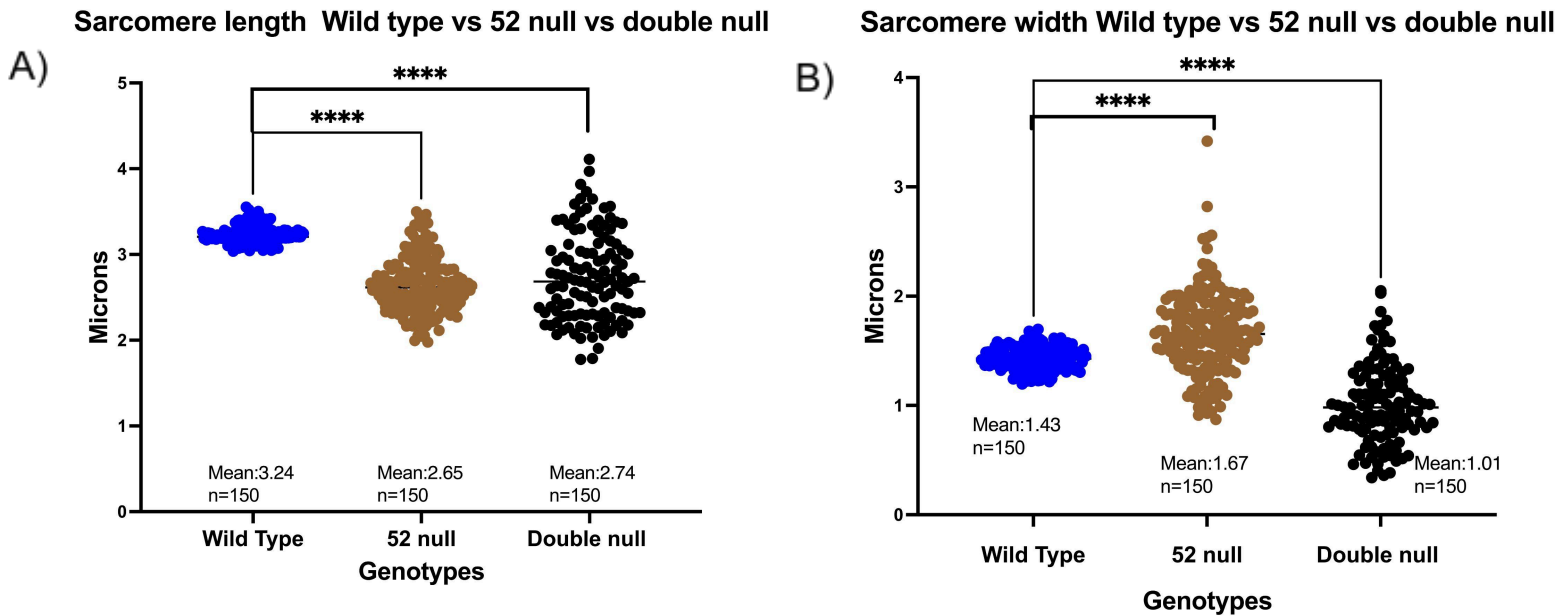
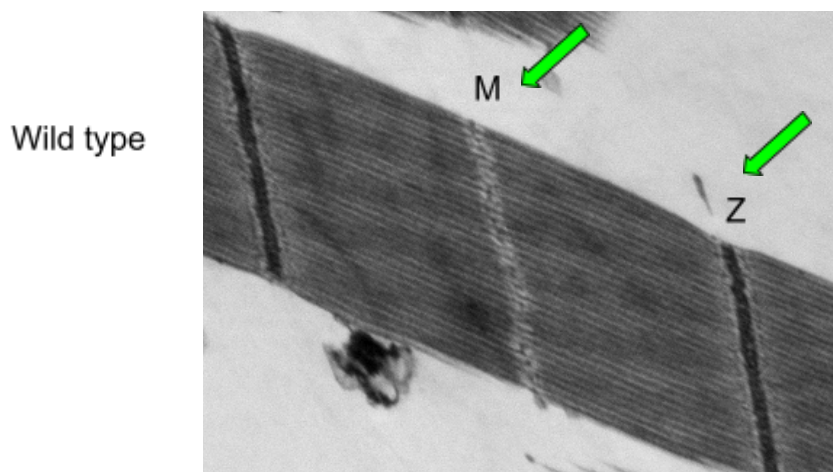


Figure 19: Plot of sarcomere quantifications for null mutant assays generated in

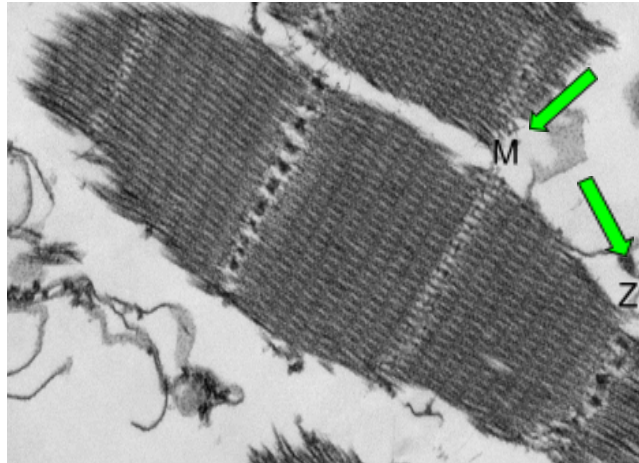
PRISM, A: Sarcomere lengths B: Sarcomere widths. Sample comparison between Wild type (navy blue) with Zasp52 null mutant (brown) and Zasp52-67 double null mutant (black). P values are represented by asterisks (**), with $P < 0.0001$ indicated as “****”. Each plot represents 150 quantifications displayed as dots, with a line indicating the median.

Transmitted electron microscopy confirms the aberrant phenotypes in Zasp52 null and Zasp52-67 double null mutant.

To further characterize the Zasp null mutant phenotypes, transmission electron microscopy (TEM) was used to compare the ultrastructure of body wall muscles between wild-type and Zasp null mutants (Figure 20). The preparation protocol employed is described in the materials and methods section.



Zasp52 null



Zasp52-Zasp67
double null

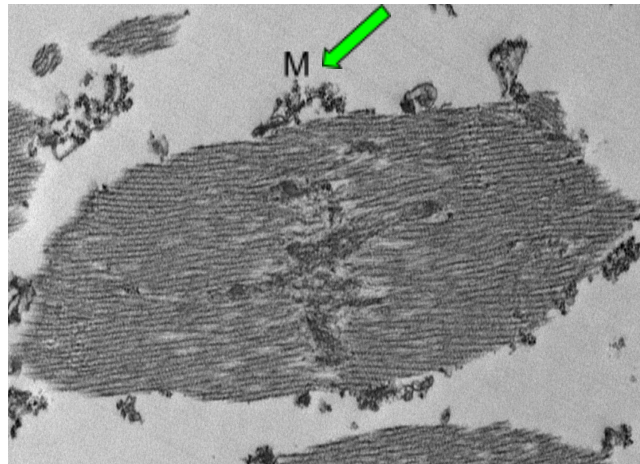


Figure 20: Transmission electron microscopy reveals detailed sarcomere defects in Zasp null mutants. Green arrows highlight the Z-discs or M-lines in each phenotype.

Zasp52-Zasp66 homozygous double null mutant and Zasp52-Zasp66-Zasp67 homozygous triple null mutant are lethal and die before third instar larvae.

To determine the developmental stage of death, the genotypes “Zasp52 null/CTG; Zasp66-Zasp67/TTG” triple null mutant and “Zasp52 null/CTG; Zasp66/TTG” double null mutant were analyzed. Here, CTG and TTG refer to GFP-marked balancer chromosomes, allowing the identification of homozygous null mutants at the embryonic stage by the absence of GFP. Following the exclusion of GFP-positive and empty embryos, the remaining GFP-negative embryos were observed every 24 hours to monitor survival. Both null mutant embryos exhibited the same survival patterns. Larvae survived for one or two days but did not reach the third day. According to the literature on the *Drosophila melanogaster* life cycle, second-instar larvae should emerge by the second day at 25°C (Roote and Prokop, 2013), consistent with this study's observations. No third instar larvae or prepupae were detected, though some embryos developed into larger larvae capable of movement on agarose plates. Consistent with previous findings, both null mutants did not produce viable survivors, confirming the lethal nature of the mutation at the embryonic or early larval stage.

General aim 2: Study the conservation of the Zasp function.

Anti-flag M2 antibody detected Flag fusion proteins in all the overexpression assays.

The Zasp52-607P>L transgene was designed to assess the functional conservation of a clinically relevant human variant in *Drosophila*. This transgene was expressed in IFMs by crossing flies with the transgenic constructs "Act88F-Gal4" and "UAS-Zasp52-607P>L." Similar methods were employed for wild-type Zasp52-PR ("UAS-Zasp52-PR") and the healthy human variant ("UAS-H-ZaspI2") as part of overexpression and rescue assays. After crossing the driver and the UAS lines, the IFMs of the progeny were dissected for analysis.

Before dissection, western blot analyses were conducted using the "Anti-Flag-M2" antibody to confirm the expression and correct fusion of the recombinant proteins. The design of the Zasp52-607P>L construct included a "Flag-strep-his-tag" fusion, allowing detection by Anti-Flag-M2. Figures 21 and 22 present the western blot results. In Figure 21, Zasp52-PR and Zasp52-PR-607P>L showed a band just above the 75 kDa marker, consistent with the predicted size of 79.46 kDa from FlyBase (A). In Figure 22, the H-ZaspI2 sample was detected just above the 63 kDa marker, which aligns with the reported 66 kDa (FlyBase B) size. Wild-type samples, which lack fusion proteins, served as negative controls and showed no bands in Figure 22.

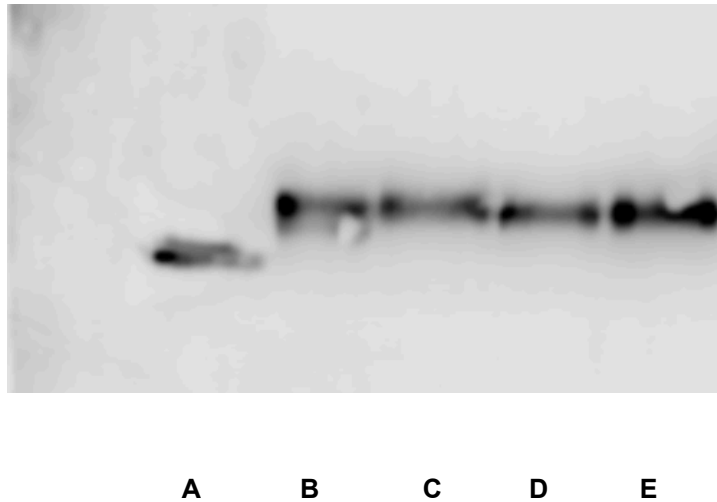


Figure 21: Western blot analysis using the Flag M2 antibody to detect Zasp52-PR and Zasp52-PR-607P>L fusion proteins. Lane A displays the protein ladder marked at 75 kDa, made visible using the western blot marker pen. Lanes B and C contain duplicate samples of Zasp52-PR, while lanes D and E contain duplicate samples of Zasp52-PR-607P>L.

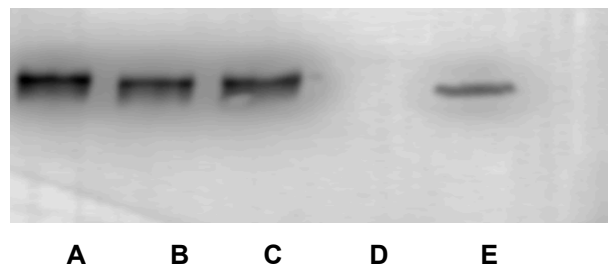


Figure 22: Western blot analysis using the Flag M2 antibody. Lane E shows the protein ladder marked at 63 kDa, made visible by the western blot marker pen.

Lane D contains a wild-type sample. Lanes A, B, and C contain Human-Zasp12 samples.

When Zasp52-PR is expressed by ACT88F-Gal4, the sarcomere presents overexpression defects, when the clinical variant “607P>L” is expressed, the phenotype worsens.

To explore the functional conservation of Zasp proteins, a *Drosophila* Zasp52 transgene harboring a clinically relevant mutation (Zasp52-PR-607P>L) was overexpressed in *Drosophila*'s indirect flight muscles (IFMs) using the Gal4-UAS system. The muscle phenotype resulting from this overexpression was compared to that of the Zasp52-PR isoform, which includes all functional domains (ZM, PDZ, LIM1-4). Figure 23 displays the phenotypes of the overexpressed proteins, showing that both the wild-type Zasp52-PR and the mutant variant Zasp52-PR-607P>L produced similar morphological outcomes: enlarged Z-discs and disrupted sarcomere organization, both distinct from the normal wild-type phenotype. Quantitative analyses were performed using PRISM to assess these qualitative observations further.

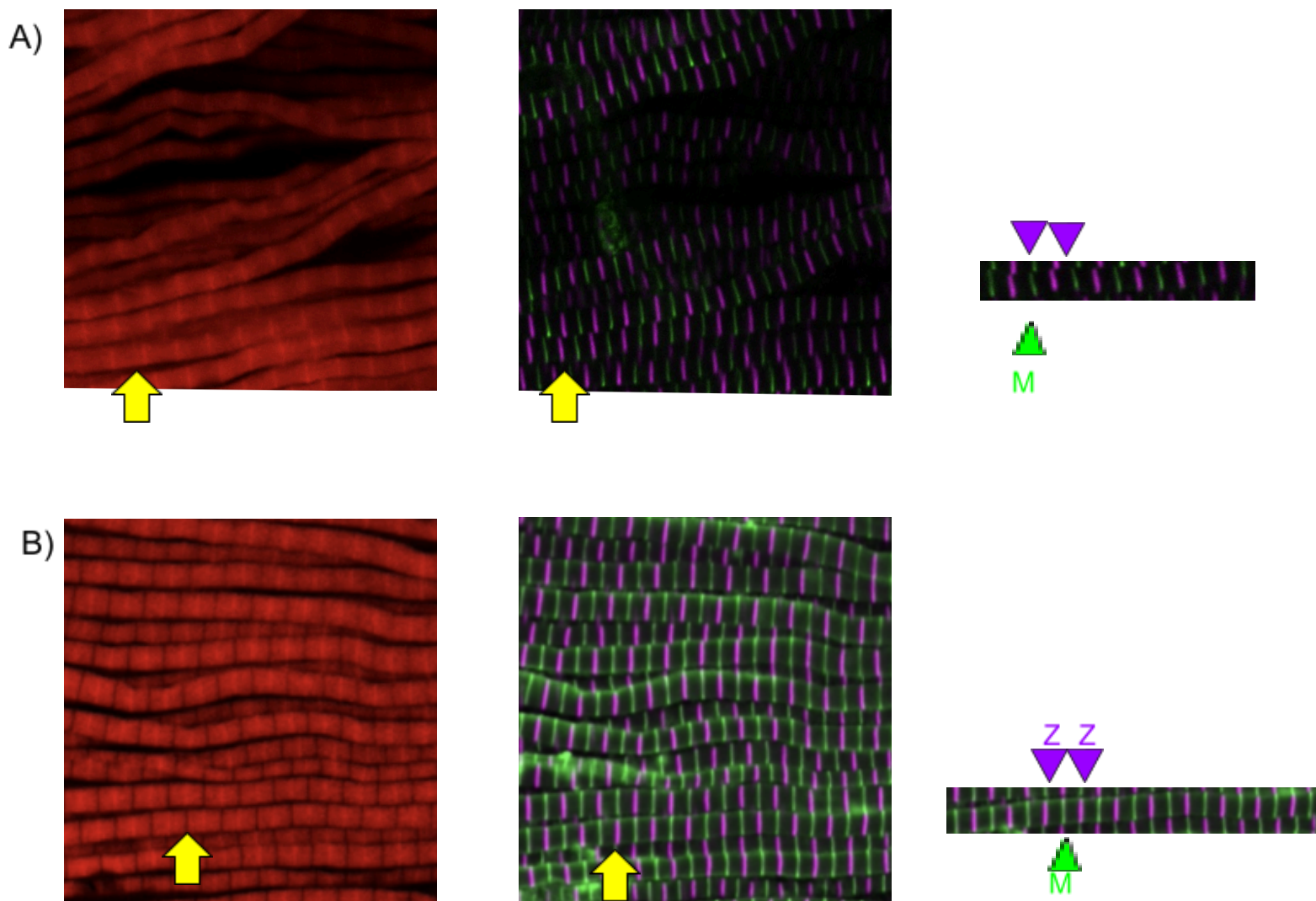


Figure 23: Confocal microscopy of the Overexpression assays. Confocal images of 5-day-old flies IFM's from different genotypes. Actin filaments are stained with phalloidin (red), anti-SIs were used to mark the Z-discs (magenta), and anti-obscurin ig 14-16 was used to mark the M-lines. **A)** Expression of Zasp52-PR under Act88F-Gal4 has an expected overexpression phenotype **B)** Overexpression of Zasp52-PR-607P>L under Act88F-Gal4 has a similar overexpression phenotype. For each sample, a single myofibril is indicated with a yellow arrow,

and on the far right, a sarcomere is highlighted with two Z-discs (magenta) and one M-line (green).

Quantifications of sarcomere length and sarcomere width on overexpression assays reveal statistically significant differences.

Figure 24 presents the full range of quantifications from the overexpression assay, including a T-test statistical analysis summary with mean values, sample sizes, and P-values. Both "sarcomere length" and "sarcomere width" show extremely significant differences (P-value = ****), indicating a substantial deviation in data behavior. The point mutation "607P>L" resulted in further increases in both sarcomere length and width. Compared to normal *Drosophila* sarcomere sizes (length: 3.2 μm , width: 1.4 μm), Zasp52-PR overexpression enlarges sarcomere length while maintaining a similar width. In contrast, Zasp52-PR-607P>L variants increase both dimensions relative to wild-type and Zasp52-PR conditions.

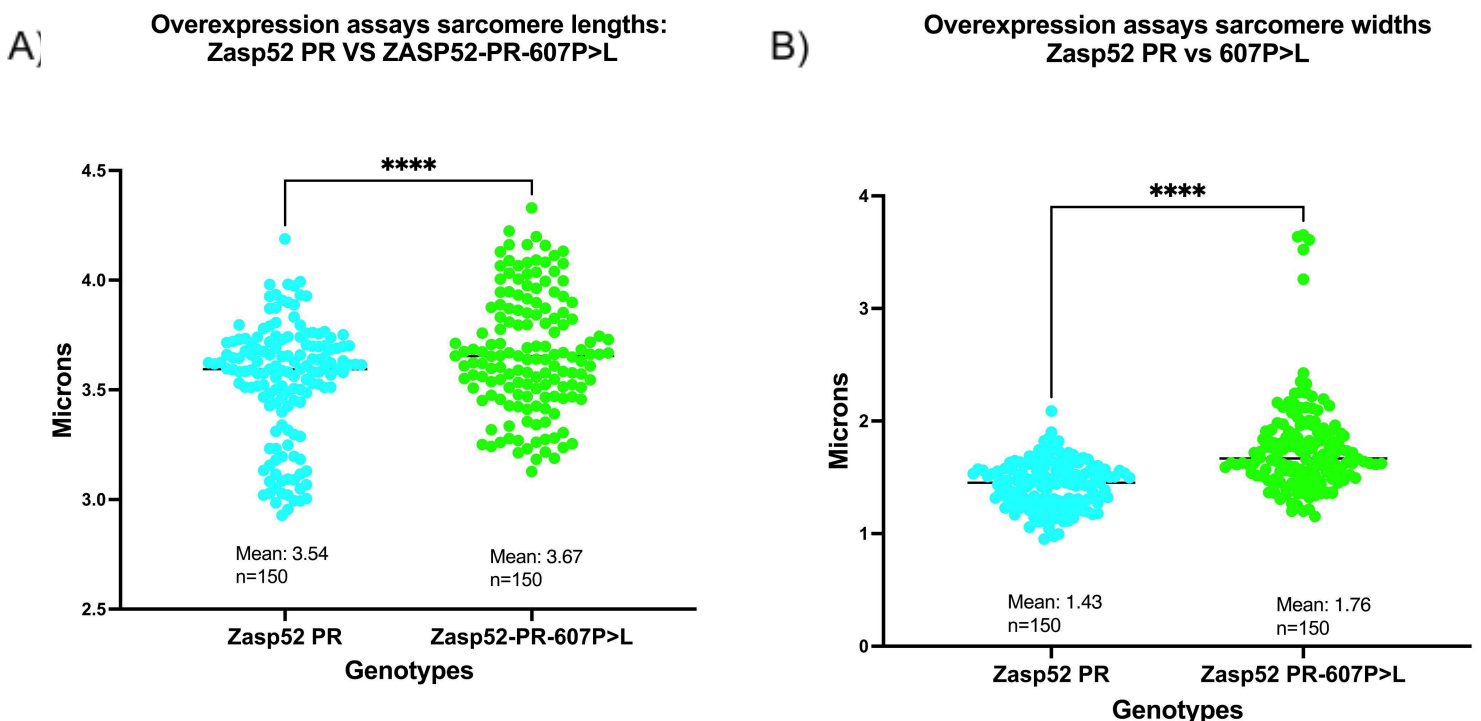


Figure 24: Plot of sarcomere quantifications for overexpression assays generated in PRISM, A: Sarcomere lengths B: Sarcomere widths. Sample comparison between Zasp52-PR (light blue) and Zasp52-PR-607P>L (green). P values are represented by asterisks (**), with $P < 0.0001$ indicated as “****”. Each plot represents 150 quantifications displayed as dots, with a line indicating the median.

Confocal microscopy reveals that the rescue assays can partially rescue the 52 null mutants when Zasp52-PR and Zasp52-PR-607P>L are overexpressed.

To further investigate the conservation of Zasp protein function, rescue assays were conducted on Zasp52 null mutant backgrounds by overexpressing different Zasp variants, including the wild-type *Drosophila* Zasp52-PR, the clinical variant Zasp52-PR-607P>L, and the wild-type human Zasp I2. The aim was to determine whether these variants could restore the myofibril structure towards a wild-type phenotype. Figure 25 shows the qualitative analysis of these rescue assays. Overexpression of Zasp52-PR and Zasp52-PR-607P>L improved the Zasp52 null phenotype, as some myofibrils (indicated by yellow arrows) displayed a more consistent diameter and reduced undulations compared to the Zasp52 null myofibrils shown in Figure 18-B. However, myofibrils remained frayed in the rescue assays involving Human-ZaspI2 and showed limited structural improvement. A quantitative analysis of sarcomere dimensions will be conducted to assess the extent of the observed phenotypic rescue.

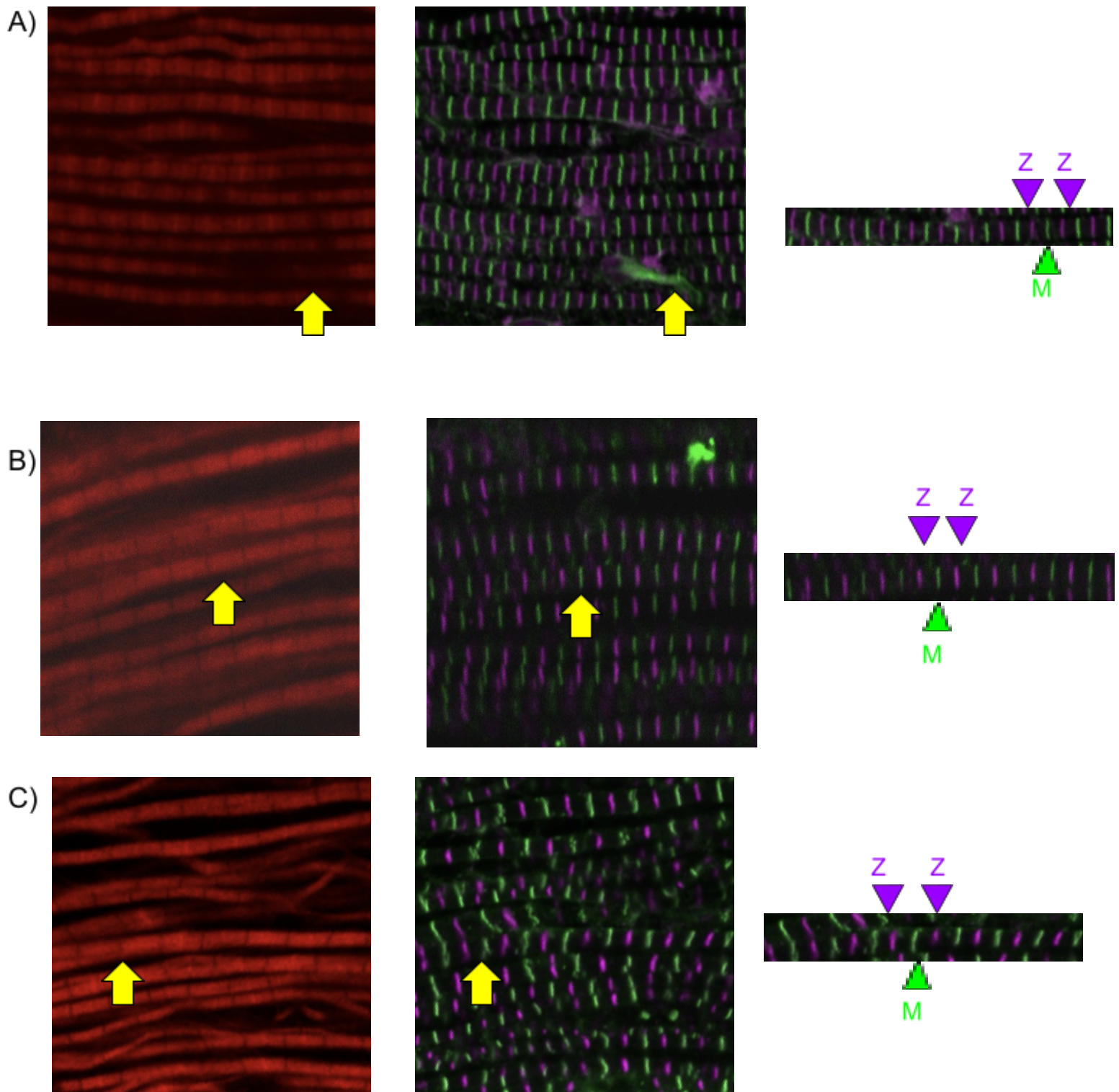


Figure 25: Confocal microscopy of the Rescue assays revealed an improvement of the phenotype in a *Zasp52* null mutant background. Confocal

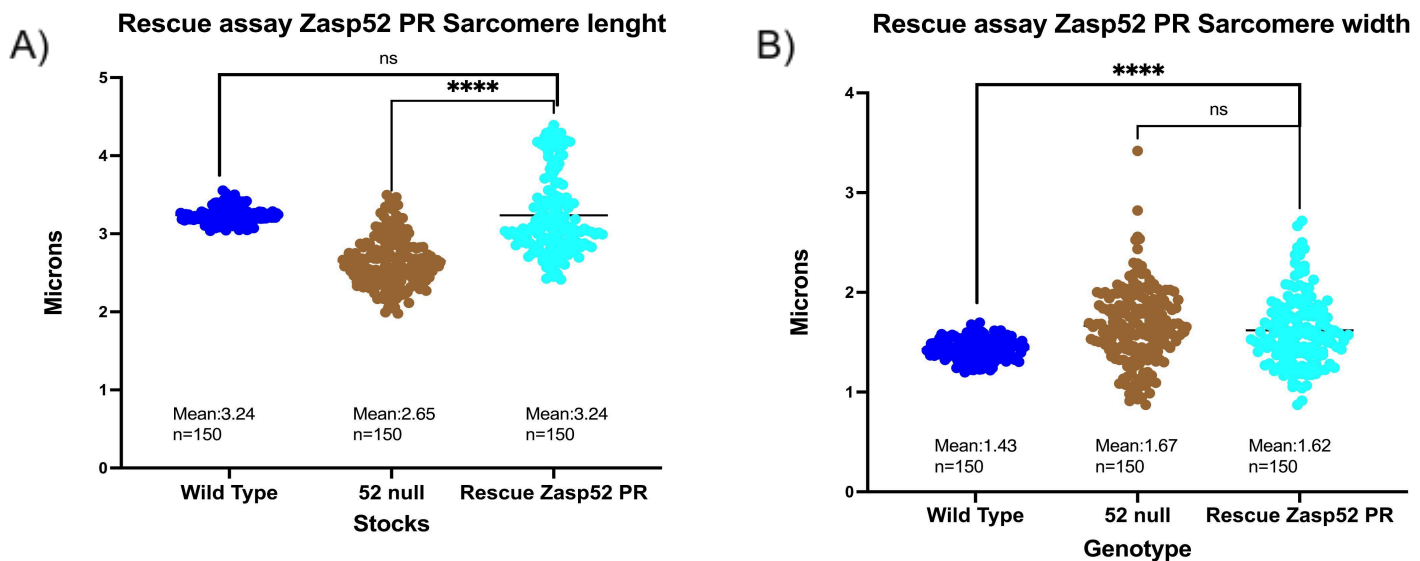
images of 5-day-old flies IFM's from different genotypes. Actin filaments are stained with phalloidin (red), anti-SIs were used to mark the Z-discs (magenta), and anti-obscurin ig 14-16 was used to mark the M-lines. A) Overexpression of Zasp52-PR under Act88F-Gal4 improves the phenotype when compared with the Zasp52 null B) Overexpression of Zasp52-PR-607P>L under Act88F-Gal4 improves the phenotype when compared with the Zasp52 null C) Overexpression of Human-ZaspI2 under Act88F-Gal4. For each sample, a single myofibril is indicated with a yellow arrow, and on the far right, a sarcomere is highlighted with two Z-discs (magenta) and one M-line (green).

Quantifications of sarcomere length and sarcomere width on rescue assays reveal myofibrils partially going back to wild-type sizes.

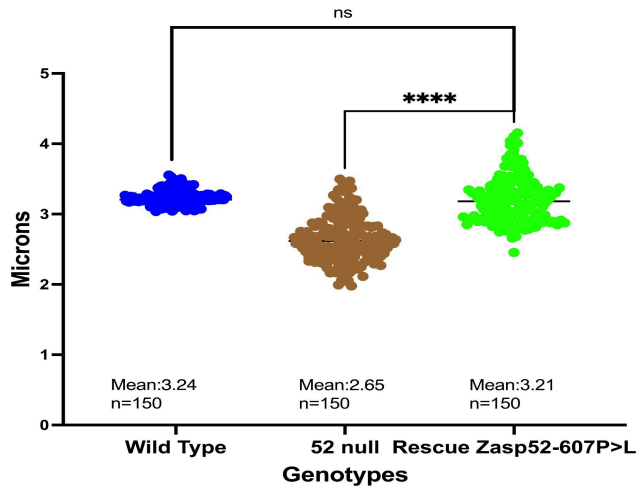
The rescue assays for Zasp52 null mutants using overexpression of Zasp52-PR, Zasp52-PR-607P>L, and Human-Zasp-I2 were quantitatively assessed to evaluate improvements in sarcomere length and width, aiming for values consistent with the wild-type phenotype. Sarcomere lengths in both Zasp52-PR and Zasp52-PR-607P>L rescues were similar to the wild type, with no significant differences (wild type: 3.24 microns, Zasp52-PR: 3.21 microns, Zasp52-PR-607P>L: 3.21 microns), as shown in Figures 26-A and 26-C. In contrast, sarcomere widths for both Zasp52-PR (1.62 microns) and Zasp52-PR-607P>L (1.35 microns) deviated significantly from the wild type (1.43 microns), with the Zasp52-PR assay showing closer resemblance to the Zasp52 null mutant (1.67 microns). At the same time, the Zasp52-PR-607P>L results

suggested less deviation from the wild type, although differences remained significant ($P < 0.001$).

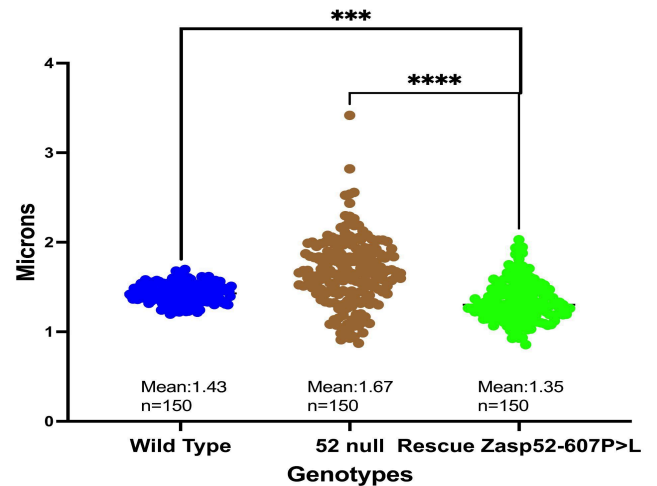
The Human-Zasp-I2 rescue did not return sarcomere dimensions to wild-type ranges, as extremely significant differences were observed for length and width (Figure 26-E, 26-F). Despite this, the Human-Zasp-I2 overexpression yielded a distinct myofibril appearance compared to the Zasp52 null phenotype. This effect is evident in Figure 26-C, where the Zasp52 null mutants show frayed sarcomeres. Still, the human Zasp-I2 overexpression displays a unique structural alteration that, while not reflective of wild-type myofibrils, suggests a species-specific interaction with the *Drosophila* myofibril components.



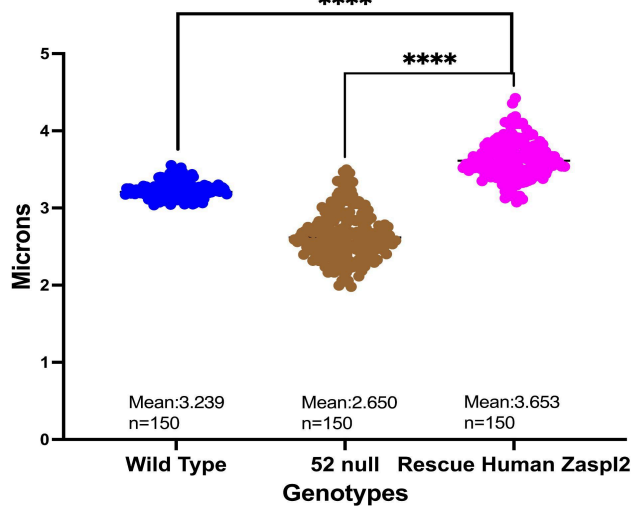
C) Rescue assay Zasp52 PR-607P>L Sarcomere lenght



D) Rescue assay Zasp52PR-607P>L Sarcomere Width



E) Rescue assay Human Zasp12 Sarcomere lenght



F) Rescue assay Human Zasp12 Sarcomere width

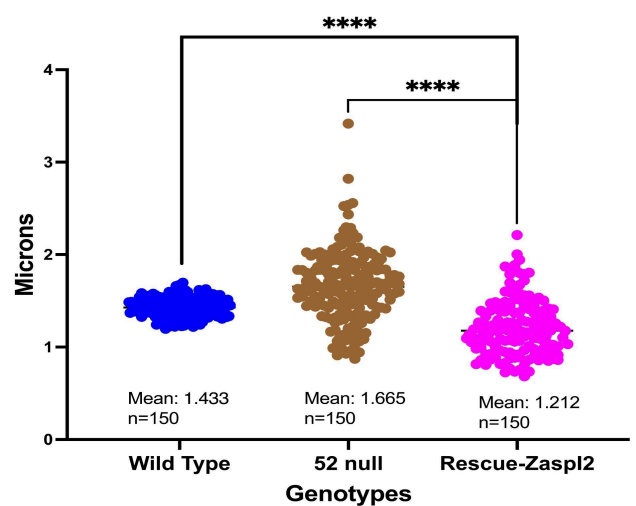


Fig 26: Plot of sarcomere quantifications for rescue assays in 52 null mutant contexts generated in PRISM, A, C, E: Sarcomere lengths B, D, F: Sarcomere widths. Each rescue assay was compared with wild type (Navy blue) and 52 nulls (Brown). The different expressed proteins for phenotype rescue were: Zasp52-PR (A-B, Light blue), Zasp52-PR-607P>L (C-D, Green), and Human-Zasp12 (E-F, Pink). P values are represented by asterisks (**), with $P < 0.0001$ indicated as ****.

“****” - “Extremely significant”.

Yeast two-hybrid assays revealed an increase in binding affinity in Zasp52-PR-607P>L.

Y2H assays were conducted using LIM2b3, LIM2b34, and their 607P>L mutant variants to assess their binding affinity with the Zasp66 ZM domain. This specific binding LIM domain binding pattern (Exon 17 instead of 16, see Figure 1-D) was selected as the sequence had less self-activation (False positives) in previous Y2H assays. Figures 27 and 28 present data from these assays, including control experiments with empty prey and bait plasmids. As shown in Figures 27-28A, no or very limited growth was observed on -WLH or -WLHA media for Zasp66 co-transformed with the empty prey pGBK plasmid when diluted, indicating limited nonspecific activation of the reporter genes. Even in the undiluted assay section (UD), there was only growth in the “-WLH + 5mm 3AT” constructs with the point mutation.

The wild-type constructs exhibited limited growth on the selective media, with few colonies in both assays: “Lim2b3” and “Lim2b34” (Figure 27-B, Figure 28-B). In contrast, the 607P>L mutation constructs showed notable differences in growth patterns compared to the wild-type LIM constructs in deficient media (Figures 27-B and 28-B).

The mutated constructs in the -WLHA + 5mM 3AT assays (Figure 28-B) observed very significant interaction activity, which supports the hypothesis that the

607P>L mutation influences the binding affinity of LIM domains to Zasp66. Notably, LIM2b34607P>L exhibited the most consistent growth on the -WLHA media, suggesting this combination and mutation may have the highest binding affinity in the presence of 3AT, even under high-stringency conditions.

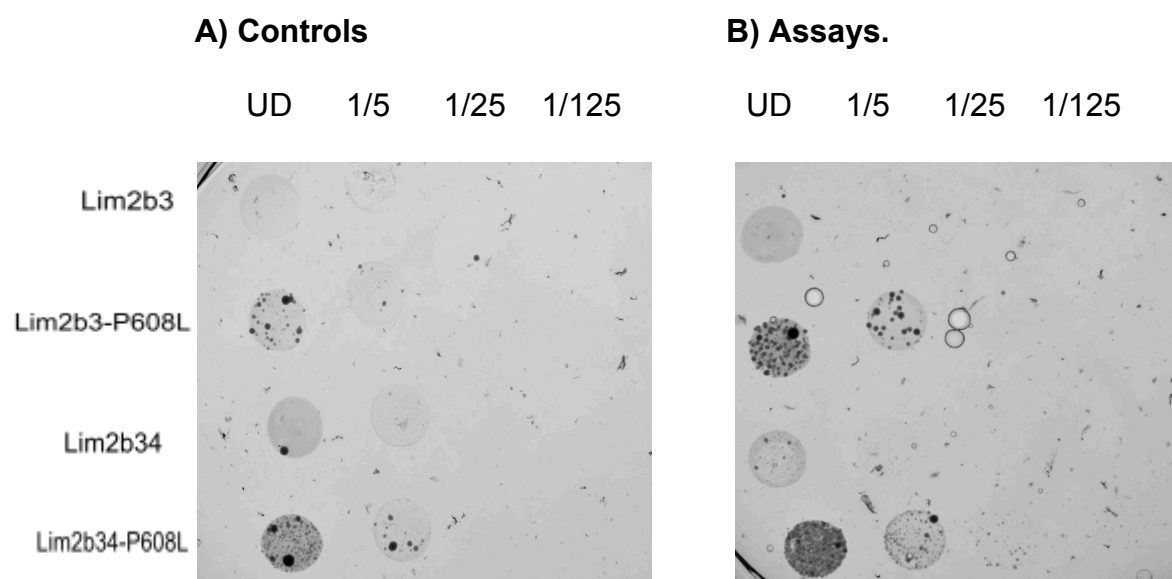


Fig 27: 1/5 serial dilutions of Y2H cultured in -WLH + 5mm 3AT.

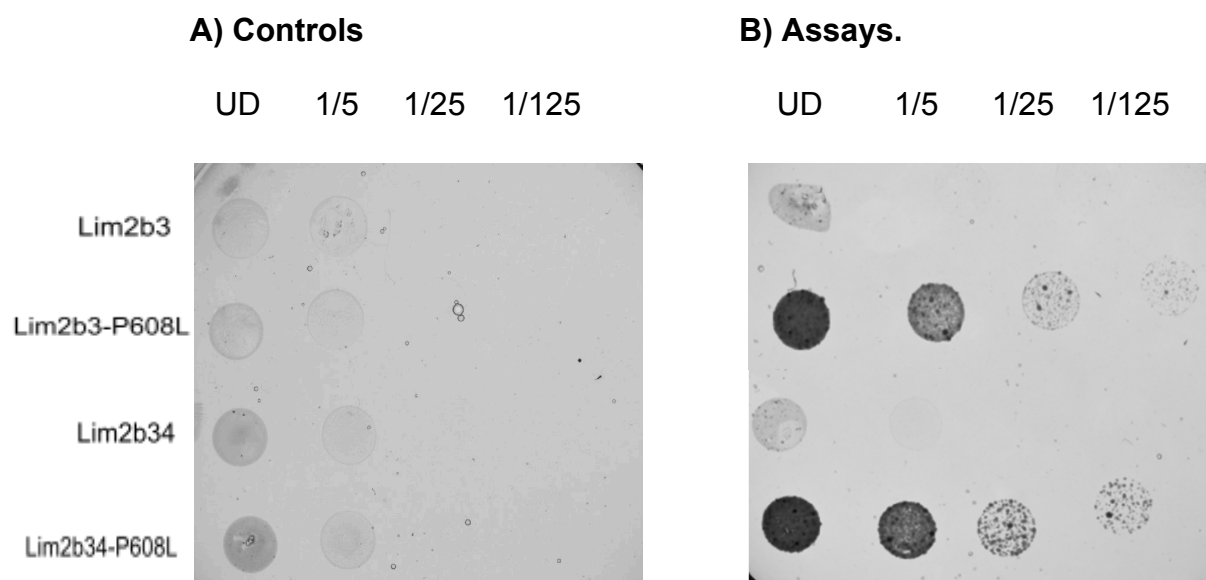


Fig 28: 1/5 serial dilutions of Y2H cultured in -WLHA + 5mm 3AT.

Discussion

The present work was developed around the research question: How do null mutations in the *Drosophila* Zasp family, along with the introduction of a human clinical variant in *Drosophila*, affect muscle development, function, and integrity, and to what extent do these findings demonstrate the conservation of molecular mechanisms between *Drosophila* and humans? This research question encompasses two general aims: The design and analysis of Zasp null mutants, and the study of the conservation of Zasp function.

In our study of Zasp null mutants, we found that the Zasp52 null mutation severely impacts *Drosophila* IFMs, and this phenotype is notably exacerbated in the Zasp52-Zasp67 double null mutation. Rescue assays in the Zasp52 null mutant, where Zasp52-PR was expressed in the IFMs, improved the phenotype, confirming that the null mutation specifically caused the defects. Our results underscore significant conservation between *Drosophila* and human muscle biology, as the human clinical Zasp variant 608P>L, when replicated in *Drosophila* Zasp52, demonstrated conserved pathological effects in IFMs. Furthermore, we developed an overexpression system for analyzing conserved point mutations in Zasp, distinguishing wild-type and disease-related phenotypes. This system showed that 607P>L increased sarcomere length and width, as supported by immunostaining and quantitative analysis. Yeast two-hybrid assays revealed increased binding affinity between Zasp52 mutated LIM domains with Zasp ZM, suggesting a molecular mechanism for the mutation's effects.

This work demonstrates the successful generation of a Zasp52 null mutant that removes all isoforms. The strategy employed here—using two rounds of CRISPR deletion combined with FRT site and fluorescent marker insertions—proved effective for targeting a complex gene with multiple splice variants. The absence of GFP and RFP markers preliminarily confirmed complete gene deletion. Subsequent validation through western blot analysis with a Zasp-Full-length antibody further corroborated the null mutation. As this antibody overlaps significantly with all isoforms, this result ensures comprehensive detection, revealing no protein bands.

Additionally, PCR showed no Zasp52 amplicon, while Zasp66 and Zasp67 were successfully amplified, validating specificity. A Zasp52-Zasp67 double null mutant was also developed and confirmed by PCR. Both mutants offer critical insights into Zasp's role in muscle development across wild-type, diseased, and mutated conditions.

The progressive worsening of the myofibril phenotype from Zasp52 null to Zasp52-Zasp67 double null mutants aligns with the hypothesis that combined mutations of Zasp proteins lead to more severe muscle defects beyond the additive effects of single mutations, as supported by previous studies. Both mutants showed sarcomere measurements that differed significantly from the wild type, consistent with earlier findings by Katzemich *et al.* (2013) and González-Morales *et al.* (2019a), who detailed *Drosophila* Zasp expression profiles. Their RNAseq and mRNA data indicated that early-stage expression of Zasp52 growing isoforms, such as Zasp52-PR, begins around 24 hours APF, while isoforms restricting Z-disc

growth, like Zasp52 Isoform 1, appear later around 60 hours APF. These temporal patterns likely influence sarcomere formation, as Z-bodies emerge around 36 hours APF (Orfano *et al.*, 2015). Zasp52 and Zasp66 exhibit similar expression profiles across developmental stages, peaking in the puparium, while Zasp67 expression is restricted to puparium stages. This context explains the pronounced phenotype in double null mutants, as the remaining Zasp66 alone cannot sustain IFM integrity. Meanwhile, the viability of both mutants may be due to Zasp66's compensatory role during pupal development, supporting essential functions despite Zasp52 and Zasp67 absence. The disrupted myofibril structure in Zasp52-Zasp67 double null mutants highlights the Zasp family's critical role in myofibril assembly and maintenance.

This analysis supports that the reduced sarcomere dimensions observed in the Zasp52-Zasp67 double null mutant result from the lack of Zasp growing isoforms. With only Zasp66 remaining—lacking LIM domains and acting as a blocking isoform—the ZM/LIM ratio shifts towards Z-disc reduction. These findings align with González-Morales *et al.* (2019b), who observed that hypomorphic Zasp52 LIM isoform mutants and overexpressed blocking isoforms, Zasp66 and Zasp67, both led to smaller Z-discs. While their study emphasized sarcomere width, a decrease in Z-disc size also likely impacts sarcomere length.

The findings in the Zasp52 null mutant reveal a more complex phenotype than initially expected, with the sarcomere length mean showing a predictable decrease while the sarcomere width mean is unexpectedly larger than the wild type. This discrepancy suggests that the influence of Zasp isoforms on sarcomere

width might require more data for precise characterization, perhaps due to inherent biological variability. González-Morales, *et al.* (2019b) got consistent results, the higher expression on growing isoforms: bigger Z-discs, and the higher expression on blocking isoforms: smaller Z-discs. However, in their work, they classified sarcomere width quantifications in different block sizes, the vast majority of their wild-type (control) width quantifications were in the range of 1.4-1.8 microns. In this way, the outlier width sizes of this range were the ones that determined if there was a stronger influence of either the blocking or the growing isoforms. In contrast, in my dataset, my control stays in a very close range of 1.4 microns. The mean of my Zasp52 null mutant width “1.67 microns” would be classified by the authors to be in the same range of the control sizes, on the other hand, the mean of 1.01 of the double null mutant would be classified by both works as significantly reduced sarcomere widths. For consistency in the future, we will follow the same data classification as the published works to either confirm the previous hypothesis or further propose adjustments. Additionally, automated software for precise sarcomere measurements will likely improve analysis accuracy. Alternatively, the increased sarcomere width of Zasp52 null mutants could also be entirely consistent with Gonzalez-Morales 2019 if we assume a more significant contribution of the short Zasp52 isoforms compared to the LIM-containing isoforms (both are deleted in our Zasp52 null mutants).

The observed larval-lethality in the triple null mutant aligns with expected outcomes based on prior studies of Zasp52-Zasp66 hypomorphic and Zasp66-Zasp67 double null mutations, both of which resulted in partial first-instar

larval lethality (Katzemich *et al.*, 2013; González-Morales *et al.*, 2019a). Other studies have also underscored the role of Zasp52 during early development. For instance, Ashour *et al.* (2023) demonstrate that Zasp52 reinforces tissue integrity in embryos via supracellular actomyosin networks. It has also been suggested previously that Zasp proteins contribute to Z-disc formation by forming multiprotein complexes with α -actinin, which is crucial for muscle integrity and viability (Fisher & Schock, 2022). Given this background, it was expected that there would be no adult escapers in the Zasp triple null mutant. As Zasp52 and Zasp66 share overlapping roles in both embryonic and pupal myofibril assembly, the absence of both proteins likely exacerbates developmental defects, precluding survival beyond early larval stages, probably by functional failure in multiple striated muscle types. The next step involves examining muscle assembly in embryos with the triple null mutation, particularly focusing on α -actinin localization. If myofibril function and Z-disc recruitment of α -actinin are completely disrupted, this would support the hypothesis that the Zasp protein family is a central organizer of the Z-disc in *Drosophila*.

Insights into the conservation of Zasp function confirm that *Drosophila* can serve as a rapid model for studying disease variants of the ALP/Enigma protein family. In González-Morales *et al.* (2019b), similar mechanisms of myofibril size regulation were observed between *Drosophila* and vertebrates, as demonstrated by expressing a human Zasp isoform in *Drosophila* IFMs. Specifically, when UAS-human ZaspI1 was overexpressed with Act88F-Gal4, it caused an increase in myofibril size, mirroring the effects of wild-type Zasp52 overexpression. Following

these findings, the next step involved further demonstrating conservation by engineering Zasp52 transgenes with mutations found in human patients, such as Zasp52-PR-607P>L. The highly regular sarcomere structure in *Drosophila* IFMs makes this model particularly suited for detecting even subtle phenotypic changes. As expected, overexpressing Zasp52-PR produced an overexpression phenotype with increased sarcomere length due to an altered LIM/ZM ratio. It was hypothesized that the 607P>L mutation might affect the phenotype differently, restoring wild-type size, further increasing Z-disc size, or causing aggregate formation. The resulting disease phenotype demonstrated a significant increase in sarcomere length and width, providing clear evidence that this point mutation has a noticeable effect on *Drosophila* IFMs.

To investigate a potential molecular mechanism underlying the observed phenotype, we utilized a yeast two-hybrid (Y2H) assay, hypothesizing that the 607P>L mutation—located between the LIM2 and LIM3 domains—alters binding affinity with Zasp52 binding partners. The Y2H assay results provide evidence suggesting that the 607P>L point mutation affects the binding affinity between Zasp LIM domain constructs and Zasp66. The most substantial evidence for this alteration appears in the -WLHA + 5mM 3AT assay, where constructs with the 607P>L mutation consistently demonstrated higher growth than their wild-type counterparts. Schöck & González-Morales (2022) outline three essential steps in Z-disc assembly: crosslinking by α -actinin, the establishment of a scaffolding center by Zasp proteins, and Z-disc growth mediated by direct binding of Zasp proteins through their ZM and LIM domains. Since the Zasp LIM domains do not

interact directly with actin or α -actinin, and LIM2-LIM3 are associated with growing isoforms, the effect of 607P>L likely pertains to the final assembly step, specifically impacting Zasp protein oligomerization (Szikora *et al.*, 2020).

Zasp66's ZM domain was assessed for binding changes, drawing from studies of myopathy-related mutations. This study confirms that the 607P>L mutation significantly increases binding affinity, which could account for the observed enlarged sarcomeres. Similar findings include those of Cassandrini *et al.* (2020), who documented a clinical case in which a patient with myopathy had a point mutation in the Zasp PDZ motif (C76T). Muscle biopsy revealed that this variant increased Zasp expression and led to defects such as Z-line enlargement and aggregate formation, as observed through TEM. Arimura *et al.* (2004) also identified a DCM-causing human Zasp mutation, D626N, in the third LIM domain, which increased binding affinity with PKC. The authors proposed that this stronger binding limited PKC availability for other proteins, contributing to DCM. In this study's context, the molecular mechanism suggested is that the 607P>L mutation may extend the activity of growing isoforms, which are typically downregulated at the later stages of Z-disc formation, resulting in sarcomere overgrowth and aggregation.

The rescue experiments linked the two main research objectives to confirm that the observed Zasp52 null phenotype resulted from the complete loss of Zasp52 function and to evaluate the potential for Zasp variants to restore normal muscle structure. Previous studies (Liao *et al.*, 2016) and the abundance of splice variants suggested that only partial rescue would be achievable. However, the

significant phenotypic improvement observed with the overexpression of the Zasp52-PR isoform confirms that the observed null mutant effects are attributable to Zasp52 deletion rather than off-target mutations. Future research could explore rescuing the phenotype with longer isoforms, such as Zasp52-PI (FlyBase ID: FBpp0290528), which is 1271 aa long compared with 722 aa of Zasp52-PR. The additional disordered regions in Zasp52-PI may contain elements that could further enhance the phenotypic rescue.

Interestingly, the Zasp52-PR-607P>L variant, despite being a disease-associated mutation, also contributed to phenotypic improvement. This supports the hypothesis that the point mutation increases the binding affinity of longer isoforms, leading to a prolonged presence of growing isoforms, which, in a Zasp52 null mutant background, may help restore sarcomere dimensions closer to wild-type sizes.

Conversely, overexpression of human Zasp isoform two did not result in the same improvement as Zasp52-PR. However, it produced a different phenotype, demonstrating a high functional conservation level between Zasp52 and human Zasp. Although time constraints limited this study to Human-Zaspl2 (Uniprot: O75112-2), the true ortholog of Zasp52-PR is Human-Zaspl1 (Uniprot: O75112-1), which is a longer isoform (617 aa vs 727 aa). Future experiments with Human-Zaspl1 may yield rescue results more closely aligned with those obtained from Zasp52-PR. As a final remark, it is essential to mention that the overexpression of mutants in a wild-type background may yield more relevant results than rescue experiments because rescue experiments alter the balance of

isoforms somewhat unpredictably (both growing and blocking isoforms are deleted in the Zasp52 null). In contrast, in overexpression, only one isoform is expressed in addition to the wild-type mix of growing and blocking isoforms.

Following the demonstration of our overexpression assay to identify the P>L608 disease phenotype, the next steps will involve testing the other three-point mutations in conserved amino acids that are known to cause disease: V55I, A147V, and T213I (Sheik *et al.*, 2007). This research has the potential to be expanded to investigate human Zasp variants of unknown significance reported in ClinVar. Although approximately 570 such variants exist, the most promising candidates should meet the following criteria:

1. A two-star review status in ClinVar (indicating evidence from multiple records).
2. Association with a muscle disease (e.g., myofibrillar myopathy).
3. Classification as a single nucleotide variant.
4. Conservation of the affected amino acid position between human Zasp and *Drosophila* Zasp52.

Based on these criteria, an initial set of 12 mutations could be prioritized for assessment: R16H, P26S, L27P, D47N, V49L, T113M, R127K, R148K, E157K, R178W, R547W, and A698S, all of which are linked to myofibrillar myopathy. The conserved amino acid positions for these mutations can be observed in Figures 3 and 4 (not specifically highlighted). Depending on the results, other variants with less stringent criteria (e.g., one-star review status) could also be considered for

analysis. Future overexpression studies will focus on mutated versions of Zasp52, as these yielded better results than experiments expressing human Zasp isoforms. However, an intriguing avenue for further research involves the use of human Zasp1 instead of Zasp12 for rescue experiments. Additionally, to compare the overexpression phenotypes of wild-type human Zasp1 and the Zasp1-P608L variant.

Conclusion.

This study marks a significant step toward understanding the conserved roles of the Zasp protein family in both *Drosophila* and vertebrates. By designing and characterizing the deletion of Zasp52, the most critical gene of this family, we laid the groundwork for analyzing the *Drosophila* Zasp triple null mutant. With this new model, our lab is uniquely positioned to explore the interactions between actinin, actin, and Zasp52 at the Z-disc, unveiling the broader, redundant roles of the Zasp family—key insights for the muscle research field. Moreover, this work sheds light on the mechanisms of Z-disc-associated diseases. By analyzing the Zasp52-PR-607P>L variant, we've established a rapid evaluation system for Alp/Enigma mutations linked to various myopathies. Beyond “Human-Zasp 608P>L,” at least three additional human mutations are now known to cause muscle diseases. Looking forward, we aim to test clinical variants likely affecting

Zasp's oligomerization or binding with actinin and actin. Further research into the Zasp family will expand our understanding of its members and allow for identifying new disease-causing variants among the hundreds cataloged in the ClinVar database. This work lays the foundation for a new chapter in the study of the Zasp protein family.

References.

- 1 Abmayr, S.M.; Erickson, M.S.; Bour, B.A. Embryonic development of the larval body wall musculature of *Drosophila melanogaster*. *Trends Genet.* 1995, 11, 153–159. [CrossRef]
- 2 Arimura, T., Hayashi, T., Terada, H., Lee, S. Y., Zhou, Q., Takahashi, M., ... & Kimura, A. (2004). A Cypher/ZASP mutation associated with dilated cardiomyopathy alters the binding affinity to protein kinase C. *Journal of Biological Chemistry*, 279(8), 6746-6752.
- 3 Arndt V, Dick N, Tawo R, Dreiseidler M, Wenzel D, Hesse M, et al. Chaperone-assisted selective autophagy is essential for muscle maintenance. *Curr Biol* 2010;20(2):143-8.
- 4 Ashour, D. J. (2021). The Role of Zasp52 in the Morphogenesis of the *Drosophila melanogaster* Embryo [Apollo - University of Cambridge Repository]. <https://doi.org/10.17863/CAM.76589>
- 5 Bang, M. L., Bogomolovas, J., & Chen, J. (2022). Understanding the molecular basis of cardiomyopathy. *American Journal of Physiology-Heart and Circulatory Physiology*, 322(2), H181-H233.
- 6 Bate, M. The embryonic development of larval muscles in *Drosophila*. *Development* 1990, 110, 791. [PubMed]
- 7 Bouaouina, M., Jani, K., Long, J. Y., Czerniecki, S., Morse, E. M., Ellis, S. J., et al. (2012). Zasp regulates integrin activation. *J. Cell Sci.* 125, 5647–5657. doi:10.1242/jcs.103291
- 8 Bryantsev, A. L., Baker, P. W., Lovato, T. L., Jaramillo, M. S., & Cripps, R. M. (2012). Differential requirements for Myocyte Enhancer Factor-2 during adult myogenesis in *Drosophila*. *Developmental biology*, 361(2), 191-207.

- 9 Burton, P. M. (2008). Insights from diploblasts; the evolution of mesoderm and muscle. *J. Exp. Zool. B Mol. Dev. Evol.* 310, 5-14. doi:10.1002/jez.b.21150 Carlsson, L., Yu, J. G., Moza, M., Carpén, O. and Thornell, L. E. (2007).
- 10 Cassandrini, D., Merlini, L., Pilla, F., Cenni, V., Santi, S., Faldini, C., ... & Sabatelli, P. (2021). Protein aggregates and autophagy involvement in a family with a mutation in Z-band alternatively spliced PDZ-motif protein. *Neuromuscular Disorders*, 31(1), 44-51.
- 11 Caufield, J. H., Sakhawalkar, N., & Uetz, P. (2012). A comparison and optimization of yeast two-hybrid systems. *Methods*, 58(4), 317-324.
- 12 Chechenova, M.B., A.L. Bryantsev, and R.M. Cripps. 2013. The *Drosophila* Z-disc protein Z(210) is an adult muscle isoform of Zasp52, which is required for normal myofibril organization in indirect flight muscles. *J. Biol. Chem.* 288:3718-3726.
- 13 Cheng, H., Zheng, M., Peter, A. K., Kimura, K., Li, X., Ouyang, K., et al. (2011). Selective deletion of long but not short Cypher isoforms leads to late-onset dilated cardiomyopathy. *Hum. Mol. Genet.* 20, 1751–1762. doi:10.1093/hmg/ddr050
- 14 Ciglar, L.; Furlong, E.E. Conservation and divergence in developmental networks: A view from *Drosophila* myogenesis. *Cell Differ. Cell Div. Growth Death* 2009, 21, 754–760. [CrossRef]
- 15 Dubreuil, R.R., and P. Wang. 2000. Genetic analysis of the requirements for alpha-actinin function. *J. Muscle Res. Cell Motil.* 21:705-713.
- 16 Duff, R.M.; Tay, V.; Hackman, P.; Ravenscroft, G.; McLean, C.; Kennedy, P.; Steinbach, A.; Schöffler, W.; Van Der Ven, P.F.M.; Fürst, D.O.; et al. Mutations in the N-terminal actin-binding domain of filamin C cause a distal myopathy. *Am. J. Hum. Genet.* 2011, 88, 729–740. [Google Scholar] [CrossRef] [PubMed] [Green Version].
- 17 FlyBase(A). (n.d.). FlyBase Transcript Report: DMEL\ZASP52-RR.
<https://flybase.org/reports/FBtr0329912.htm#pubs>
- 18 Fisher, L. A., & Schöck, F. (2022). The unexpected versatility of ALP/Enigma family proteins. *Frontiers in Cell and Developmental Biology*, 10, 963608.
- 19 Frank, D., Kuhn, C., Katus, H. A., & Frey, N. (2006). The sarcomeric Z-disc: a nodal point in signaling and disease. *Journal of molecular medicine*, 84, 446-468.

- 20 Franzini-Armstrong, C., & Porter, K. R. (1963). The Z disc of skeletal muscle fibrils. *Zeitschrift für Zellforschung und mikroskopische Anatomie*, 61, 661-672.
- 21 Fratev, F., Mihaylova, E., & Pajeva, I. (2014). Combination of genetic screening and molecular dynamics as a useful tool for identification of disease-related mutations: ZASP PDZ domain G54S mutation case. *Journal of Chemical Information and Modeling*, 54(5), 1524-1536.
- 22 Fyrberg, E., M. Kelly, E. Ball, C. Fyrberg, and M.C. Reedy. 1990. Molecular genetics of *Drosophila* alpha-actinin: mutant alleles disrupt Z disc integrity and muscle insertions. *J. Cell Biol.* 110:1999-2011.
- 23 Garcia-Lopez, A., Monferrer, L., Garcia-Alcover, I., Vicente-Crespo, M., Alvarez-Abril, M. C., & Artero, R. D. (2008). Genetic and chemical modifiers of a CUG toxicity model in *Drosophila*. *PloS one*, 3(2), e1595.
- 24 García-López, A.; Llamusi, B.; Orzáez, M.; Pérez-Payá, E.; Artero, R.D (2011). In vivo discovery of a peptide that prevents CUG-RNA hairpin formation and reverses RNA toxicity in myotonic dystrophy models. *Proc. Natl. Acad. Sci. USA* 2011, 108, 11866–11871.
- 25 González-Morales, N., T.W. Marsh, A. Katzemich, O. Marescal, Y.S. Xiao, and F. Schöck. 2019a. Different Evolutionary Trajectories of Two Insect-Specific Paralogous Proteins Involved in Stabilizing Muscle Myofibrils. *Genetics*. 212:743-755.
- 26 González-Morales, N., Y.S. Xiao, M.A. Schilling, O. Marescal, K.A. Liao, and F. Schöck. 2019b. Myofibril diameter is set by a finely tuned mechanism of protein oligomerization in *Drosophila*. *Elife*. 8:e50496. See the attached paper.
- 27 Griggs, R., Vihola, A., Hackman, P., Talvinen, K., Haravuori, H., Faulkner, G., ... & Udd, B. (2007). Zaspopathy in a large classic late-onset distal myopathy family. *Brain*, 130(6), 1477-1484.
- 28 Gunage, R. D., Dhanyasi, N., Reichert, H., & VijayRaghavan, K. (2017, December). *Drosophila* adult muscle development and regeneration. In *Seminars in cell & developmental biology* (Vol. 72, pp. 56-66). Academic Press.
- 29 Iuso, A., Wiersma, M., Schüller, H.-J., Pode-Shakked, B., Marek-Yagel, D., Grigat, M., et al. (2018). Mutations in PPCS, encoding phosphopantothienoylcysteine synthetase, cause

- autosomal-recessive dilated cardiomyopathy. *Am. J. Hum. Genet.* 102, 1018–1030.
doi:10.1016/j.ajhg.2018.03.022
- 30 Jani, K., and F. Schöck. 2007. Zasp is required for the assembly of functional integrin adhesion sites. *J. Cell Biol.* 179:1583-1597.
 - 31 Johar, S. S., & Talbert, J. N. (2017). Strep-tag II fusion technology for the modification and immobilization of lipase B from *Candida antarctica* (CALB). *Journal of Genetic Engineering and Biotechnology*, 15(2), 359-367.
 - 32 Katzemich, A., Long, J. Y., Jani, K., Lee, B. R., & Schöck, F. (2011). Muscle type-specific expression of Zasp52 isoforms in *Drosophila*. *Gene Expression Patterns*, 11(8), 484-490.
 - 33 Katzemich, A., K.A. Liao, S. Czerniecki, and F. Schöck. 2013. Alp/Enigma family proteins cooperate in Z-disc formation and myofibril assembly. *PLoS Genet.* 9:e1003342.
 - 34 Knöll, R., Buyandelger, B., & Lab, M. (2011). The sarcomeric Z-disc and Z-discopathies. *BioMed Research International*, 2011(1), 569628.
 - 35 Krcmery, J., Gupta, R., Sadleir, R. W., Ahrens, M. J., Misener, S., Kamide, C., et al. (2013). Loss of the cytoskeletal protein Pdlm7 predisposes mice to heart defects and hemostatic dysfunction. *PLoS ONE* 8, e80809. doi:10.1371/journal.pone.0080809
 - 36 Liao, K. A., González-Morales, N., & Schöck, F. (2016). Zasp52, a core Z-disc protein in *Drosophila* indirect flight muscles, interacts with α -actinin via an extended PDZ domain. *PLoS genetics*, 12(10), e1006400.
 - 37 Liao, K. A., Gonzalez-Morales, N., & Schöck, F. (2020). Characterizing the actin-binding ability of Zasp52 and its contribution to myofibril assembly. *PLoS One*, 15(7), e0232137.
 - 38 Lin, X., Ruiz, J., Bajraktari, I., Ohman, R., Banerjee, S., Gribble, K., ... & Mankodi, A. (2014). Z-disc-associated, alternatively spliced, PDZ motif-containing protein (ZASP) mutations in the actin-binding domain cause disruption of skeletal muscle actin filaments in myofibrillar myopathy. *Journal of Biological Chemistry*, 289(19), 13615-13626.
 - 39 Luther, P. K. (2009). The vertebrate muscle Z-disc: sarcomere anchor for structure and signaling. *Journal of muscle research and cell motility*, 30, 171-185.

- 40 Manivannan, S. N., Darouich, S., Masmoudi, A., Gordon, D., Zender, G., Han, Z., et al. (2020). Novel frameshift variant in MYL2 reveals molecular differences between dominant and recessive forms of hypertrophic cardiomyopathy. *PLoS Genet.* 16, e1008639. doi:10.1371/journal.pgen.1008639
- 41 Maqbool, T., & Jagla, K. (2007). Genetic control of muscle development: learning from *Drosophila*. *Journal of muscle research and cell motility*, 28(7), 397-407.
- 42 Migunova, E., Theophilopoulos, J., Mercadante, M., Men, J., Zhou, C., and Dubrovsky, E. B. (2021). *ELAC2/RNaseZ-linked cardiac hypertrophy in Drosophila melanogaster*. *Dis. Model. Mech.* 14, dmm048931. doi:10.1242/dmm.048931
- 43 Miyazaki, K., K. Ohno, N. Tamura, T. Sasaki, and K. Sato. 2012. *CLP36 and RIL recruit alpha-actinin-1 to stress fibers and differentially regulate stress fiber dynamics in F2408 fibroblasts*. *Exp. Cell Res.* 318:1716-1725.
- 44 Mu, Y., R. Jing, A.K. Peter, S. Lange, L. Lin, J. Zhang, K. Ouyang, X. Fang, J. Veevers, X. Zhou, S.M. Evans, H. Cheng, and J. Chen. 2015. *Cypher and Enigma homolog protein are essential for cardiac development and embryonic survival*. *J. Am. Heart Assoc.* 4:e001950.
- 45 Nikonova, E., S.Y. Kao, and M.L. Spletter. 2020. Contributions of alternative splicing to muscle type development and function. *Semin. Cell Dev. Biol.* In press.
- 46 Orfanos, Z., Leonard, K., Elliott, C., Katzemich, A., Bullard, B., & Sparrow, J. (2015). Sallimus and the dynamics of sarcomere assembly in *Drosophila* flight muscles. *Journal of Molecular Biology*, 427(12), 2151-2158.
- 47 Pashmforoush, M., P. Pomiès, K.L. Peterson, S. Kubalak, J. Ross, Jr., A. Hefti, U. Aebi, M.C. Beckerle, and K.R. Chien. 2001. Adult mice deficient in actinin-associated LIM-domain protein reveal a developmental pathway for right ventricular cardiomyopathy. *Nat. Med.* 7:591-597.
- 48 Picchio, L.; Plantie, E.; Renaud, Y.; Poovthumkadavil, P.; Jagla, K. Novel *Drosophila* model of myotonic dystrophy type 1: phenotypic characterization and genome-wide view of altered gene expression. *Hum. Mol. Genet.* 2013, 22, 2795–2810. [CrossRef] [PubMed]
- 49 Poovathumkadavil, P., & Jagla, K. (2020). Genetic control of muscle diversification and homeostasis: Insights from *Drosophila*. *Cells*, 9(6), 1543.

- 50 Pyle, W. G., & Solaro, R. J. (2004). At the crossroads of myocardial signaling: the role of Z-discs in intracellular signaling and cardiac function. *Circulation Research*, 94(3), 296-305.
- 51 QIAGEN. (s. f.-b). DNeasy Blood & Tissue Kits | DNA Purification | Qiagen.com.
<https://www.qiagen.com/us/products/discovery-and-translational-research/dna-rna-purification/dna-purification/genomic-dna/dneasy-blood-and-tissue-kit>
- 52 Rohn, J.L., D. Sims, T. Liu, M. Fedorova, F. Schöck, J. Dopie, M.K. Vartiainen, A.A. Kiger, N. Perrimon, and B. Baum. 2011. Comparative RNAi screening identifies a conserved core metazoan actinome by phenotype. *J. Cell Biol.* 194:789-805.
- 53 Roote, John, and Andreas Prokop. "How to design a genetic mating scheme: a basic training package for *Drosophila* genetics." *G3: Genes| Genomes| Genetics* 3.2 (2013): 353-358.
- 54 Rubin GM (2001) The draft sequences. Comparing species. *Nature* 409(6822):820–821
- 55 Sanger, J. W., Kang, S., Siebrands, C. C., Freeman, N., Du, A., Wang, J., ... & Sanger, J. M. (2005). How to build a myofibril. *Journal of Muscle Research & Cell Motility*, 26, 343-354.
- 56 Schöck, F., & González-Morales, N. (2022). The insect perspective on Z-disc structure and biology. *Journal of Cell Science*, 135(20), jcs260179.
- 57 Seipel, K. and Schmid, V. (2005). Evolution of striated muscle: jellyfish and the origin of triploblasty. *Dev. Biol.* 282, 14-26. doi:10.1016/j.ydbio.2005.03.032
- 58 Selcen, D., & Engel, A. G. (2011). Myofibrillar myopathies. *Handbook of clinical neurology*, 101, 143-154.
- 59 Sheikh, F., Bang, M. L., Lange, S., & Chen, J. (2007). "Z" eroing in on the role of Cypher in striated muscle function, signaling, and human disease. *Trends in cardiovascular medicine*, 17(8), 258-262.
- 60 Sparrow, J.; Reedy, M.; Ball, E.; Kyrtatas, V.; Molloy, J.; Durston, J.; Hennessey, E.; White, D. Functional and ultrastructural effects of a missense mutation in the indirect flight muscle-specific actin gene of *Drosophila melanogaster*. *J. Mol. Biol.* 1991, 222, 963–982. [
- 61 Sparrow, J.C., and F. Schöck. 2009. The initial steps of myofibril assembly: integrins pave the way. *Nat. Rev. Mol. Cell Biol.* 10:293-298.

- 62 Spletter, Maria L., et al. "A transcriptomics resource reveals a transcriptional transition during ordered sarcomere morphogenesis in flight muscle." *Elife* 7 (2018): e34058.
- 63 Steinmetz, P.R.H., J.E.M. Kraus, C. Larroux, J.U. Hammel, A. Amon-Hassenzahl, E. Houliston, G. Wörheide, M. Nickel, B.M. Degnan, and U. Technau. 2012. Independent evolution of striated muscles in cnidarians and bilaterians. *Nature*. 487:231-234.
- 64 Szikora, S., Gajdos, T., Novák, T., Farkas, D., Földi, I., Lenart, P., Erdélyi, M. and Mihály, J. (2020). Nanoscopy reveals the layered organization of the sarcomeric H-zone and I-band complexes. *J. Cell Biol.* 219, e201907026. <https://doi.org/10.1083/jcb.201907026>
- 65 Ugur, B., Chen, K., and Bellen, H. J. (2016). *Drosophila* tools and assays for the study of human diseases. *Dis. Model. Mech.* 9, 235–244. doi: 10.1242/dmm.023762
- 66 Vatta, M., Mohapatra, B., Jimenez, S., Sanchez, X., Faulkner, G., Perles, Z., ... & Towbin, J. A. (2003). Mutations in Cypher/ZASP in patients with dilated cardiomyopathy and left ventricular non-compaction. *Journal of the American College of Cardiology*, 42(11), 2014-2027.
- 67 Wadmore, K., Azad, A. J., & Gehmlich, K. (2021). The role of Z-disc proteins in myopathy and cardiomyopathy. *International Journal of Molecular Sciences*, 22(6), 3058.
- 68 Zhao, Yunpo, Joyce van de Leemput, and Zhe Han. "The opportunities and challenges of using *Drosophila* to model human cardiac diseases." *Frontiers in Physiology* 14 (2023): 1182610.
- 69 Zheng, M., H. Cheng, I. Banerjee, and J. Chen. 2010. ALP/Enigma PDZ-LIM domain proteins in the heart. *J Mol Cell Biol.* 2:96-102.